TABLE OF CONTENTS

LIST OF FIGURES

LIST OF TABLES

LIST OF ABBREVIATIONS

μl	microliter
1,1-DCE	1,1,-Dichloroethene
40 CFR	Title 40 Code of Federal Regulations
cis-DCE	Cis-1,2-dichloroethene
DNAPL	Dense Nonaqueous Phase Liquid
EPA	Environmental Protection Agency
k_{MV}	Mass and volume normalized rate constant (L g^{-1} hr^{-1})
k_{SA}	Surface area normalized rate constant (L $hr^{-1}m^{-2}$)
mg	milligram
ml	milliliter
ppm	parts per million
PRBW	Permeable Reactive Barrier Wall
TCE	Trichloroethene
trans-DCE	Trans-1,2-dichloroethene

INTRODUCTION

Chlorinated solvents, such as trichloroethylene (TCE), are toxic and persistent environmental pollutants. TCE is used in many industrial applications, mainly as a degreaser in many metal manufacturing processes. These solvents enter soil and groundwater when released through improper disposal practices. Once released, TCE will readily migrate through the subsurface soil and into the groundwater. These chlorinated solvents have higher densities than water and are collectively referred to as dense nonaqueous phase liquids (DNAPLs). Due to their relatively high densities, DNAPLs will continue to sink through the groundwater until they reach a non-permeable surface such as bedrock. The DNAPLs will form a pool that slowly dissolves into the groundwater, creating a down gradient contaminant plume (Figure 1). The solubility of TCE in water is 1.1×10^3 mg/L (ECAO, 1985, as cited in Nyer, 1996). This relatively low solubility causes the TCE pool to remain present for very long periods of time. Depending on the flow rate of the groundwater, the contaminated plume can diffuse for large distances, possibly into sources of drinking water.

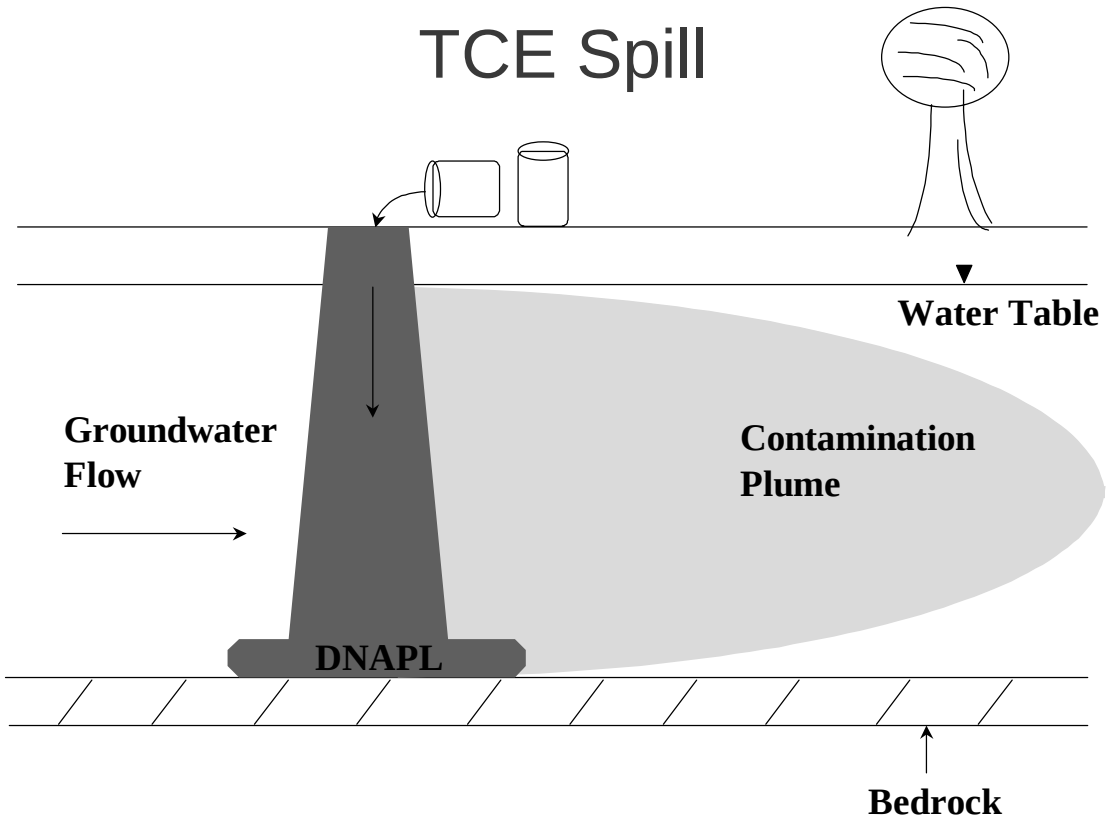

Figure 1. Contamination plume from a TCE spill (Lau, 1998).

The Environmental Protection Agency (EPA) approximates that there are 5000 Department of Energy, Department of Defense, and Superfund sites contaminated with chlorinated solvents (1996). Due to this widespread contamination, the EPA has established a maximum contaminant level of TCE acceptable in groundwater of 4 μg/L (USEPA 40CFR Part 134). To meet these guidelines, sites are forced to employ at least one of several available remediation techniques.

Pump and Treat Remediation

TCE contaminated sites are most commonly remediated through the use of pumps to remove groundwater from the subsurface so it can be treated above ground. The treatment usually involves carbon adsorption or air stripping to remove TCE from the water. The effluent from these processes must then be transported to a wastewater treatment plant or pumped again into the ground.

There are several drawbacks to this traditional type of remediation. Among these drawbacks are cost and effectiveness. The initial cost of equipment and the cost of manpower to maintain the equipment are high. The method involves multiple pumps as well as a surface plant to treat the contaminated water. This equipment needs to be maintained often to achieve optimal performance and lifetime. The lifetime of the equipment is limited, and replacement due to failure may be necessary. The effectiveness of pump and treat remediation decreases over time. Although the initial TCE depletion rates can be high, these rates decrease over time due to diffusion effects. This causes the TCE concentration of the effluent to increase, sometimes to values that are above regulatory levels.

Permeable Reactive Barrier Wall Remediation

An alternative method of remediating TCE contaminated groundwater is the use of a permeable reactive barrier wall (PRBW). The use of this technology has gained popularity in recent years and has been the focus of many research projects. The PRBW is installed across the path of a contaminated plume. The construction of the wall

involves alternating sections of impermeable sheet piling with permeable sections consisting of a mixture of sand and reactive iron material. This process contains the contaminated groundwater and a preferential flow through a path of least resistance is created. As the contaminated groundwater flows through the wall, TCE is degraded, producing a decontaminated plume on the down gradient side of the wall (Figure 2).

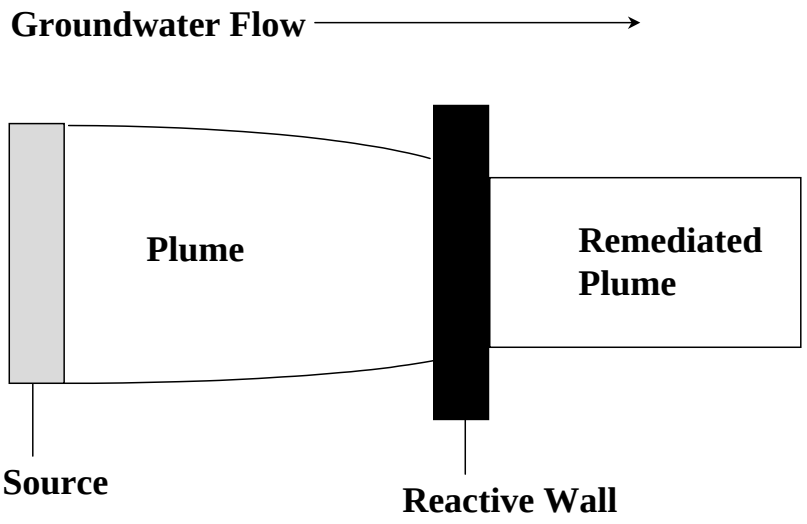

Figure 2. Schematic representation of a permeable reactive barrier wall (Ruiz, 1998).

The use of zero-valent metals, such as iron, to effectively reductively dechlorinate DNAPLs has been employed as the reactive material in these PRBWs (Gillham et al.,

1993). PRBW technology is advantageous to traditional pump and treat methods in several ways. The initial installation costs are much less due to the lack of mechanical equipment. Without the use of mechanical equipment, the possibility of failure is eliminated, thus reducing long-term costs. TCE degradation rates of a PRBW decrease over time, mainly due to the formation of precipitates that prevent TCE from coming into contact with the reactive iron surface. Recent studies suggest that the application of ultrasound to rejuvenate the PRBW by removing these precipitates can be effective. Sonication removes obstructive material from an iron surface and improves its activity for the degradation of chlorinated solvents and is effective even in water environments with a great tendency to form precipitates (Ruiz, 1998).

Zero-Valent Metal Technology

Zero-valent metals have been proven to effectively degrade chlorinated aliphatics (Gillham and O'Hannesin, 1992). Because of iron's low cost and low toxicity, the mechanisms and reaction rates at which iron reduces chlorinated aliphatics have been studied extensively (Gillham and O'Hannesin, 1993, Lau, 1998). The half reaction in Equation 1 has a reduction potential of –0.440 V (Brown, Lemay, and Bursten, 1994). The estimated standard reduction potentials of alkyl halides at a pH of 7, as in Equation 2, ranges from +0.5 to +1.5 V (Vogel, Cridle, and McCarty, 1987). Therefore, the net reaction in Equation 3 is thermodynamically favorable (Hudlicky, 1984 and House, 1972, as cited by Matheson and Tratnyek, 1994).

$$Fe^{0} \rightarrow Fe^{2+} + 2e^{-} \quad (1)$$

$$\underline{RX + 2e^{-} + H^{+} \rightarrow RH + X^{-}} \quad (2)$$

$$Fe^{o} + RX + H^{+} \rightarrow Fe^{2+} + RH + X^{-} \quad (3)$$

The reductive dehalogenation of alkyl halides by iron metal is a corrosive process as can be seen by these equations.

Although the mechanistic pathway for the degradation of TCE is not precisely known, three potential pathways have been proposed by Matheson and Tratnyek (1994). The first proposed pathway is shown in Figure 3. This pathway occurs by direct electron transfer from the surface of the iron to the alkyl halide. Equation 4 describes this pathway.

Direct Reduction at Surface of Iron Particle

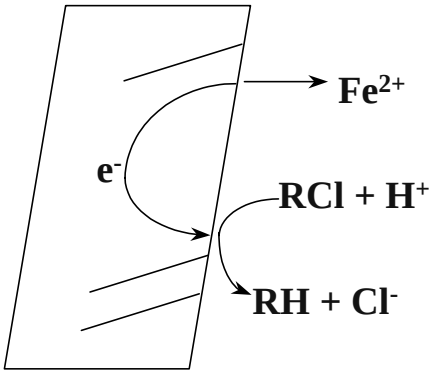

Figure 3. Direct electron transfer at the iron surface (Matheson and Tratnyek, 1994)

$$Fe^0 + RX + H^+ \rightarrow Fe^{2+} + RH + X^- \quad (4)$$

The second proposed pathway is displayed in Figure 4. This pathway involves the production of Fe^{2+} resulting from the corrosion of the metal. The Fe^{2+} is then reduced to Fe^{3+} through the transfer of electrons to the alkyl halide. Equation 5 describes the reaction that is thought to take place.

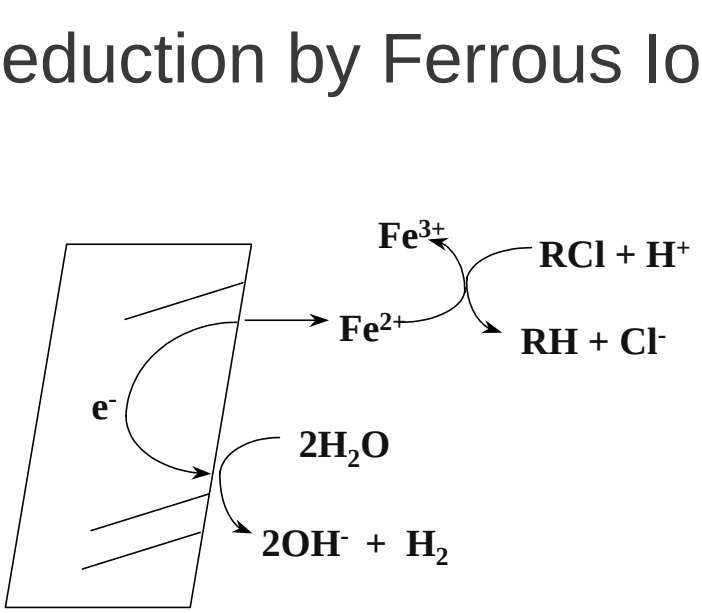

Figure 4. Reduction by Fe^{2+} that results from metal corrosion (Matheson and Tratnyek, 1994).

$$2Fe^{2+} + RX + H^{+} \rightarrow 2Fe^{3+} + RH + X^{-} \quad (5)$$

The utilization of hydrogen produced from the corrosion of water is involved in the third pathway. The iron surface serves as a catalyst in the reaction (Figure 5 and Equation 6).

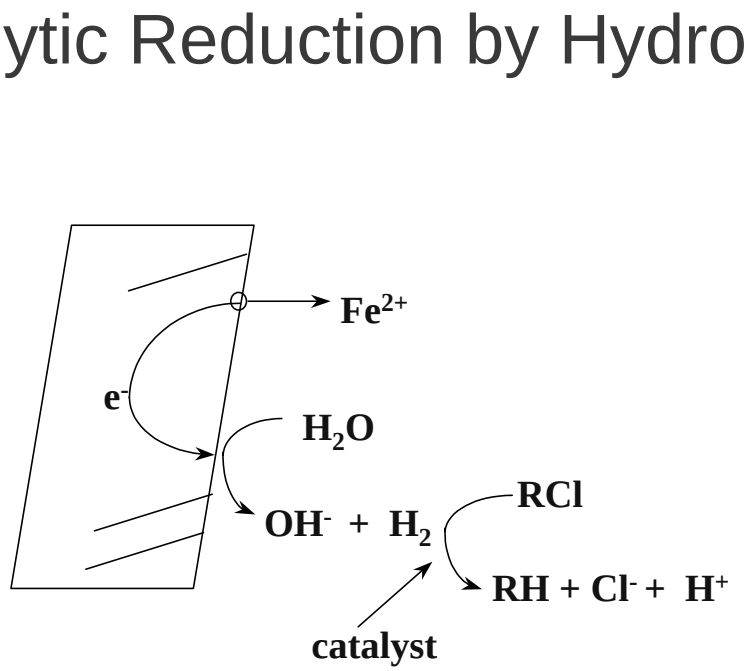

Figure 5. Catalytic reduction of the alkyl halide by hydrogen at the iron surface (Matheson and Tratnyek, 1994).

$$H_2 + RX \rightarrow RH + X^- + H^+ \qquad (6)$$

Matheson and Tratnyek (1994) have proposed the pathways of TCE dehalogenation. Hydrogenolysis occurs, where each of the three chlorines are replaced sequentially. The TCE first reduces to cis-1,2-dichloroethene, trans-1,2-dichloroethene,

and 1,1-dichloroethene. These intermediates are then reduced to vinyl chloride, ethene and ethane. Beta elimination, the replacement of two chlorides, has been suggested by Sivavec and Horney (1997) and Roberts, et al (1996) as the major pathway of TCE degradation. Both proposed pathways involve a net two-electron transfer (Figure 6).

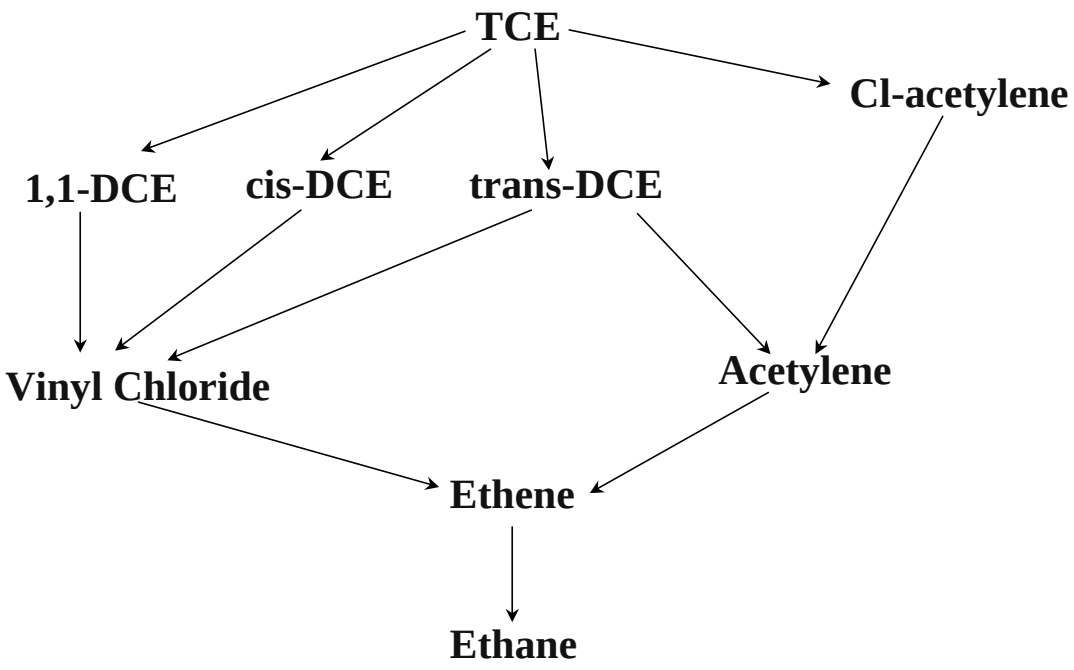

Figure 6. Possible mechanistic pathways for the reductive dehalogenation of TCE

Objectives

The objectives of this research project involved the comparisons of dehalogenation reaction rates for various types of iron particles obtained from several different sources. This required the optimization of batch vial experiments in order to obtain reliable, reproducible data so that rate constants could be compared. The optimization involved the determination of TCE concentrations and iron amounts that would produce manageable reaction rates. Once an acceptable method for obtaining rate constants was devised, the next objective was to determine the effects that several pretreatment techniques had on the rate constants. After obtaining rate constants for many different iron types and normalizing them by mass and volume, k_{MV}, the surface areas were determined for the iron types and their rate constants were normalized by surface area, k_{SA}. The objective here was to find differences in rate constants of iron types that could be related to inherent characteristics of the iron, such as composition or crystal structure, as opposed to just differences in surface area.

EXPERIMENTAL

Materials

Several types of iron from various sources were used in this experiment. Fine gray iron, ductile iron + 1% Cu, and two types of cast iron metal filings were obtained from Peerless Metal Powders and Abrasive. Iron aggregate in sizes (–8+50), 50 mesh, (-18+50), (-30+70), and (-8+20) were obtained from Connelly-GPM Inc. One to three micron 98% iron powder was obtained from Alfa Aesar. Nanoscale iron particles were synthesized in the laboratory using a modified method of Wang and Zhang, (1997). Stock chemicals included trichloroethylene (99% stabilized, Acros Organics, New Jersey, USA), and HPLC grade methanol (Fisher Scientific, Fairlawn, New Jersey, USA). Calibration standards for vinyl chloride, 1,1-dichloroethene, cis-1,2-dichloroethene, trans-1,2-dichloroethene, and trichloroethene were purchased from Absolute, Inc. at a concentration of 20,000 mg/L in methanol. Reaction vessels consisted of Quorpak 40 mL glass vials equipped with Teflon septum screw caps and 20 mL glass vials equipped with Teflon septum crimp caps.

TCE Solution Preparation

Two methods of preparing TCE solutions were utilized in this research. The first method involved dissolving a known amount of TCE in methanol followed by dilution in water to achieve a desired concentration. The second method involved preparing a saturated solution of TCE in water, then diluting an aliquot of the solution in water. To

emulate the anaerobic conditions of groundwater, all solutions were prepared using deoxygenated water in a nitrogen atmosphere glove box.

TCE / Methanol Spike

500 mL of deionized water was added to a 1000 mL Tedlar bag. The water was deoxygenated by purging with nitrogen for 30 minutes. All of the headspace was removed by collapsing the bag until the point where only liquid remained. A sample consisting of 0.3 mL of a 5000 ppm TCE/methanol solution was injected into the bag using a syringe through the bag septum to obtain approximately a 3 ppm solution of TCE in water. The sample was then tested by gas chromatography to determine the exact TCE concentration. This method introduced methanol to the solution, which was found to interfere with the chromatographic resolution of some compounds of interest. The following method was found to be just as reliable without contributing to a methanol chromatographic peak and was used for most experiments throughout this research.

Dilution of TCE Saturated Stock Solution

A saturated stock solution of TCE was prepared by adding TCE to a 4000 mL flask of deionized water until a pool of TCE formed at the bottom of the flask. The flask was placed in the hood on a magnetic stirrer and sealed with parafilm. The solution was purged with nitrogen for 60 minutes to remove any dissolved oxygen present. The solution was then allowed to equilibrate overnight. Using a 60 mL syringe with a length of tubing attached, an aliquot of the saturated solution was transferred to a Quorpak 40

mL vial and brought to the nitrogen box. Working solutions were then made by diluting 2 ml of the solution in 1000 mL of deionized, deoxygenated water. This dilution produced working solutions of approximately 3 ppm TCE. The resulting solutions were then analyzed by gas chromatography to obtain the exact concentration of TCE.

Batch Vial Experiments

Batch experiments utilized Quorpak 40 mL glass vials equipped with Teflon lined septum screw caps. Throughout the experimental setups, anaerobic conditions were maintained to emulate groundwater conditions. To achieve this, all solutions used were deoxygenated using a nitrogen gas purge and vial loading took place in a nitrogen atmosphere glove box. Various iron samples and different pretreatment techniques were used and reaction rates were compared.

Untreated Iron Samples

Iron samples, 30 Quorpak 40 mL vials per sample, and 2000 mL of a prepared deoxygenated 3 ppm TCE solution were placed in a nitrogen atmosphere glove box. A 2 gram sample of iron was weighed and added to each of 20 separate vials. The vials were filled with TCE solution to the level were there was a bead on top. The vials were capped, leaving no headspace and were checked for the presence of air bubbles. The remaining 10 vials, containing no iron, were filled and capped in the same manner and used as controls. The sample vials and control vials were removed from the glove box and placed on a shaker to prevent the formation of a concentration gradient. Periodically,

two replicate sample vials and one control vial were removed from the shaker and analyzed in duplicate by gas chromatography.

Acid Washing Iron Samples

Twenty Quorpak 40 mL vials were loaded with 2 g each of an iron sample. The vials were filled with a 5% v/v sulfuric acid/water solution and allowed to react for 30 minutes. The sample vials and 10 control vials containing no iron were brought into a nitrogen glove box and the iron was rinsed three times with deoxygenated water. The vials were filled with a 3 ppm TCE solution to the level were there was a bead on top. The vials were capped, leaving no headspace and were checked for the presence of air bubbles. The remaining 10 vials, containing no iron, were filled and capped in the same manner and used as controls. The sample vials and control vials were removed from the glove box and placed on a shaker to prevent the formation of a concentration gradient. Periodically, two replicate sample vials and one control vial were removed from the shaker and analyzed in duplicate by gas chromatography.

Sonication of Iron Samples

Twenty Quorpak 40 mL vials were loaded with 2 g each of an iron sample. The sample vials and 10 control vials containing no iron were brought into a nitrogen glove box. The vials were filled with a 3 ppm TCE solution to the level were there was a bead on top. The vials were capped, leaving no headspace and were checked for the presence of air bubbles. The remaining 10 vials, containing no iron, were filled and capped in the

same manner and used as controls. The sample vials and the control vials were placed in an ultrasonic bath for 30 minutes. The sample vials and control vials were placed on a shaker to prevent the formation of a concentration gradient. Periodically, two replicate sample vials and one control vial were removed from the shaker and analyzed in duplicate by gas chromatography.

Oxidation of Iron by Calcium Carbonate

A saturated solution of calcium carbonate was prepared to simulate groundwater effects on the iron's surface and reactivity. A 0.2 g sample of calcium carbonate was added to a 250 mL Erlenmeyer flask. The flask was brought into the nitrogen glove box, and then a 40 g sample of iron and 200 mL of deoxygenated water was added to the flask and sealed with parafilm. The sample was allowed to stand for one week. The iron was vacuum filtrated and dried under a stream of nitrogen. The samples were analyzed by SEM to visualize any surface corrosion that might have formed. The samples also underwent batch vial studies with no further treatment, with acid wash pretreatment, and with ultrasound pretreatment.

Bulk Iron Pre-treatment

Several experiments involved pre-treating iron samples before the vials were loaded. A 40 g iron sample was added to a 250 mL Erlenmeyer flask. The iron was then either acid washed or sonicated in an ultrasonic bath. The acid wash involved adding 200

mL of a 5% sulfuric acid/water solution to the flask and allowing the solution to react for 30 minutes. When sonicating samples, 200 mL of deionized water was added to the flask and placed in an ultrasonic bath for 30 minutes. Both techniques were followed by rinsing three times with deoxygenated water and drying under nitrogen in a nitrogen glove box. The iron samples were then weighed and loaded into vials for analysis as described previously.

Synthesis of Nanoscale Iron Particles

Nanoscale iron was prepared by a modified method of Wang and Zhang, 1997. A 1.6 M $NaBH_4$ aqueous solution was added dropwise to a 1.0 M $Fe_2(SO_4)_3$.$6H_2O$ aqueous solution. The reaction vessel was mixed with a magnetic stirrer at ambient temperature. Ferric iron (Fe^{3+}) was reduced to iron metal with the evolution of hydrogen (Equation 7).

$$Fe\ (H_20)_6^{3+} + 3BH_4^- + 3H_2O \rightarrow Fe^0 + 3B(OH)_3 + 10.5H_2 \quad (7)$$

The precipitated iron particles were collected by filtration in a nitrogen atmosphere, washed with deionized, deoxygenated water and dried under a stream of flowing nitrogen. The iron particles were stored in a nitrogen atmosphere glove box to prevent their exposure to oxygen.

Analytical Methods

Sample analyses utilized a Hewlett Packard 5890 Series II gas chromatograph (GC) equipped with a flame ionization detector (FID). Analyses were conducted using a SPB-624 column, manufactured by Supelco, Inc. The column was 60 m in length and had an internal diameter of 0.25 mm. The thickness of the liquid phase was 1.4 μm.

The GC oven temperature program that was used had an initial temperature of 60^{o} C for 3.0 minutes. The temperature was then ramped at 15^{o} C per minute to 180^{o} C. The final temperature of 180^{o} C was held for 5.0 minutes. Helium was used as the carrier gas, and was set at a constant linear velocity of 44.2 cm/sec by using an electronic pressure controller. Samples were introduced into the GC via a 16-position Tekmar ALS autosampler and a Tekmar 3000 purge and trap system. A Vocarb 3000 K trap, supplied by Supelco, Inc., was installed.

Table 1 lists the purge and trap conditions that were used for sample analyses.

Table 1. Purge and Trap conditions for the HP5890 GC.

Parameter	Set Point
Purge Flow	36 ml/min.
Purge time	11.0 min.
Dry Purge	0.0 min.
Desorb Temp	225^{o} C
Bake Temp	250^{o} C
MCS Bake	310^{o} C
Line Temps	100^{o} C
Valve Temp	120^{o} C
Sample Temp	35^{o} C

The HP 5890 GC was calibrated for trichloroethene and its breakdown products vinyl chloride, 1,1-dichloroethene, cis-1,2-dichloroethene, and trans-1,2-dichloroethene using an eight point external calibration curve ranging from 0.010 mg/L to 4 mg/L. Additionally, the instrument was calibrated for 4-bromofluorobenzene (4-BFB), which was used as a surrogate for all samples tested. Calibration standards for each analyte, with concentrations of 20,000 mg/L in methanol, were purchased from Absolute, Inc.. From these individual stock standards, a 100 mg/L daily working standard containing each analyte was prepared according to Equation 8.

0.0050 mL * 20,000 mg/L (Stock Solution) / 1.0 mL → 100 mg/L Working Std. (8)

Different amounts of this working standard were added to 5.0 mL of deionized water to generate the calibration standards. Equation 9 describes one example of a calibration standard preparation.

0.010 mL* 100 mg/L (Working Std.) / 5.0 mL → 0.100 mg/L Calibration Std. (9)

The instrument was also calibrated for ethene from 0.15 mg/L to 3.75 mg/L. High purity gas cylinders were used to prepare the calibration standards. An intermediate calibration standard was made by placing 14.9 mL of high purity nitrogen into a 50 mL Tedlar bag. To this bag, 0.10 mL of neat ethane was added, resulting in a 1:150 gas dilution working standard. The assumption was made that N_2 and ethane are ideal gases and volumes are additive, having no intermolecular interactions (McQuarrie and Simon, 1999). Different amounts of this working standard were added to 5.0 mL to make each calibration standard. Equations 10 and 11 describe this process.

(0.10 mL of neat ethane gas)/(15.0 mL total gas volume) → 1/150 ethene dilution (10)

0.10mL * 1/150(ethene dilution) * 1L / 1000mL * 1 mole ethene/ 24.4L * 28 g/mole atomic wgt. ethene* 1000 mg/g * 1/ 0.0050 (final volume) L → 0.15 mg/L (11)

Prior to the analysis of the calibration mixtures, the retention times of each analyte were determined individually. The chromatogram of the mixture was then compared to the chromatograms published by the manufacturer of the column. The retention times of

each analyte were recorded and used for subsequent identification of analytes in experimental samples (Table 2).

Table 2. Retention times of TCE and breakdown products for the HP5890 GC.

Compound	Retention Time (minutes)
Ethene	3.58
Vinyl Chloride	4.05
1,1-Dichloroethene	5.45
Trans-1,2-dichloroethene	6.37
Cis-1,2-dichloroethene	7.46
Trichloroethene	9.15
4-BFB (Surrogate)	12.1

The calibration curves obtained for each analyte were linear in the concentration range tested, having correlation coefficients of greater than 0.99.

Prior to sample analysis, an instrument blank containing only the surrogate 4-BFB, at a concentration of 0.20 mg/L, was run to determine that the instrument was free of contamination. Additionally, a calibration verification standard (CVS), containing 0.20 mg/L of each analyte, was run to verify that the instrument was still calibrated properly and that the retention times matched those obtained from the initial calibration. If the percent recovery of any analyte of interest was not within +/- 25% of the true value, another calibration verification standard was analyzed. If the percent recovery was again outside the acceptable range, the instrument was no longer considered calibrated and the initial calibration process was repeated. If the retention time of any analyte was not

within +/- 0.05 minutes of the time obtained from the initial calibration, the initial calibration process was repeated. The analyte concentrations of experimental samples were determined by inserting the area counts of the specific analyte into the linear equation obtained from that analyte's initial calibration curve.

Experimental samples were also spiked with the surrogate 4-BFB, resulting in a surrogate concentration of 0.20 mg/L. The surrogate recovery was monitored to determine purge efficiency of the system. During each experimental sample analysis, two replicate vials were tested. Additionally, instrument duplicates were prepared for each vial to ensure that the instrument was running precisely and the sample aliquots analyzed were representative of the entire sample (Brooks, 2000).

RESULTS AND DISCUSSION

Optimizing Batch Vial Experiments

Preliminary experiments were performed to determine appropriate values for variables such as the initial TCE concentration, amount of iron, number of vials, and time between samplings. These variables were dependent on each other as well as other factors. Therefore, trial batch experiments were performed and adjustments were made depending on the results.

The initial concentrations of TCE working solutions were determined by the linear range and detection limits of the instrumentation used for analyses. Preliminary experiments utilized TCE solutions with concentrations above 10 ppm. These concentrations saturated the instrument's trap and column and were above the linear range of the detector, thus producing poor chromatographic results. Due to the volatility of the compounds, diluting each sample introduced additional experimental error, so TCE solutions with concentrations between 3 ppm and 5 ppm were used. At these concentrations, the purge and trap had no residual TCE after each completed run. Diluting samples also brought the concentrations of degradation products below detection limits. Although changes in TCE concentration were monitored and used to obtain degradation rates, the detection of degradation products was necessary to confirm that TCE breakdown was occurring. Also, due to the volatile nature of these chlorinated solvents, exposure to the atmosphere needed to be kept to a minimum. By using the

correct range of TCE concentrations, 5 mL aliquots could be removed directly from the sample vials and quickly injected into the autosampler ports.

The amount of iron added to each vial controlled the rate at which the reaction proceeded. If not enough iron was used, 0.4 g for instance, the reaction would proceed too slowly. If too much iron was used, 10 g for instance, the reaction would proceed too quickly. Both situations created experimental problems. In the case of not enough iron being present, two problems arose. First, long periods of data gathering were required to notice any significant decrease in TCE concentration. This was a problem because although the Teflon lined screw cap vials were designed to prevent the loss of the volatile species of interest, some loss of TCE in control vials was observed. To minimize the effect of this control loss, the reaction time needed to be decreased by increasing the reaction rate. In the case of too much iron, other problems were encountered. Due to the relatively low concentration of TCE and the high reaction rate, the TCE was depleted quickly. The frequency of sample analysis that was required to obtain enough data points was not feasible. In addition, the very low TCE concentrations increased the possibility of the reaction becoming diffusion controlled. This would result in a decrease in the linearity of the rate plot and lower observed rate constants. Two grams of iron per 40 mL vial produced reaction rates that were manageable and reliable.

Using a 3 ppm-5 ppm TCE solution and 2 g of iron per 40 mL vial, 30 vials were required per batch experiment. Twenty sample vials contained iron and TCE solution and 10 control vials contained only TCE solution. Analyses of two replicate sample vials and one control vial occurred every 48 hours for 20 days for most batch experiments.

Batch experiments involving iron samples with extremely high surface areas, such as nanoscale iron, required analyses of 2 replicate sample vials and 1 control vial every 24 hours for 10 days.

First-Order TCE Degradation Rates

Once TCE concentrations were recorded over time, the data was plotted. To observe the effect that iron had on the TCE concentration, the data was first plotted as a zero-order chart (Figure 7).

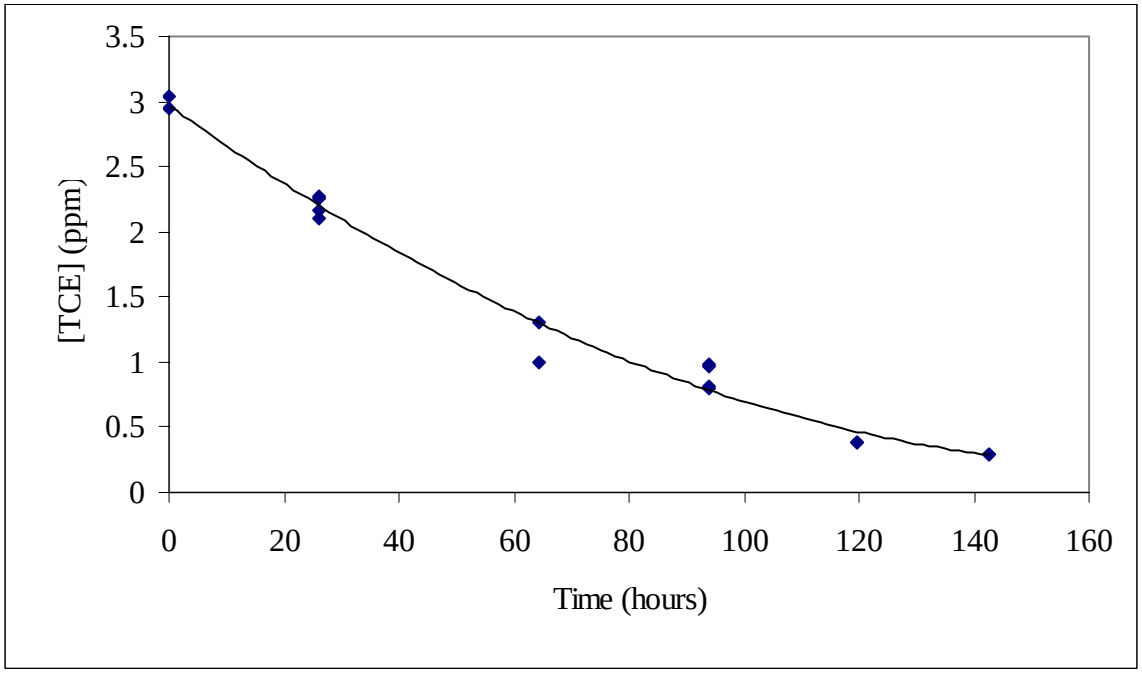

Figure 7. The change in TCE concentration with time in the presence of iron

These concentration versus time plots were not linear, and the reaction seemed to be concentration, as well as surface area, dependent. Plotting the natural log of the TCE concentration at time t over the initial TCE concentration on the y-axis, displayed linear results and it was confirmed that the reaction for TCE degradation follows first-order kinetics (Figure 8).

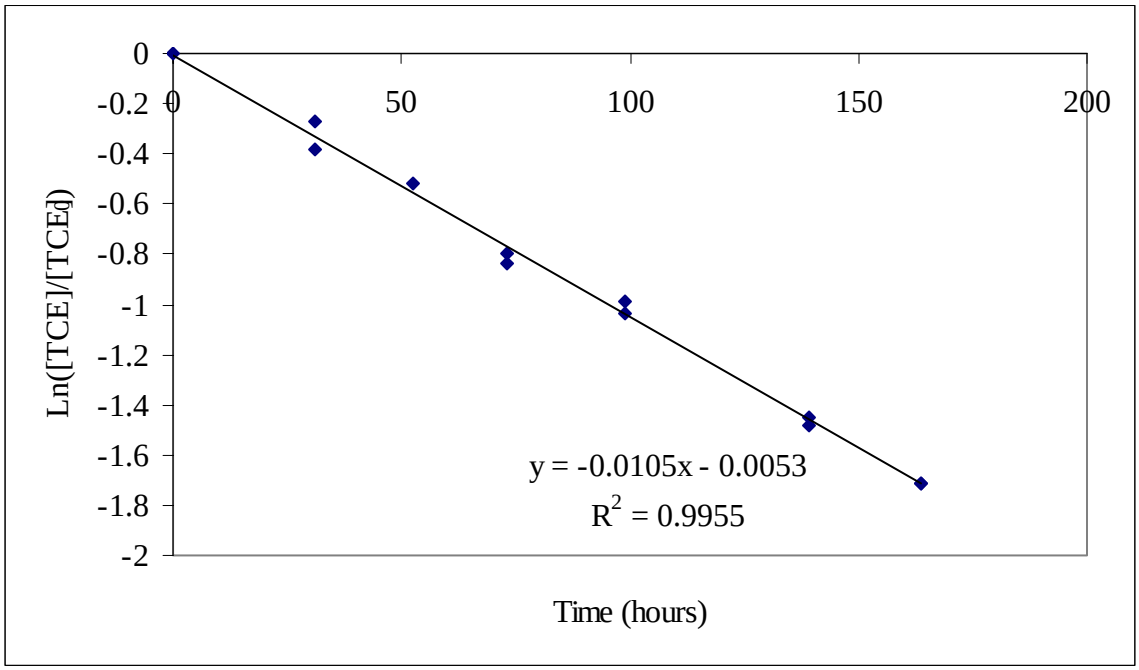

Figure 8. First order kinetics plot for TCE degradation in the presence of iron

The slope of this plot corresponds to the first order rate constant for the degradation of TCE by iron particles. It is important to note that these rate constants are specific for the reaction vessel set up used. Although these rate constants were later normalized by iron mass, it is the ratio of iron mass to TCE solution volume that controls the changes in TCE

concentration. Therefore, any comparisons of rate constants must be made using the same type of 40 mL reaction vessel or the rate constants would have to be normalized by solution volume also. Since the same type of reaction vessel was used throughout most of this research, normalization by solution volume was not necessary for the comparison of rate constants. However, so that it was clear how the rate constants were obtained and to remain consistent with rate constants reported in recent literature, (Nurmi et al., 2005), rate constants obtained in this study were normalized by iron mass and solution volume.

Since TCE depletion in reaction vials was observed, the next step was to confirm that TCE degradation was occurring. Before sampling, the vials were visually inspected for the presence of any gas bubbles. As the reaction proceeded, a gas bubble formed in the vials containing iron and grew larger over time (Figure 9).

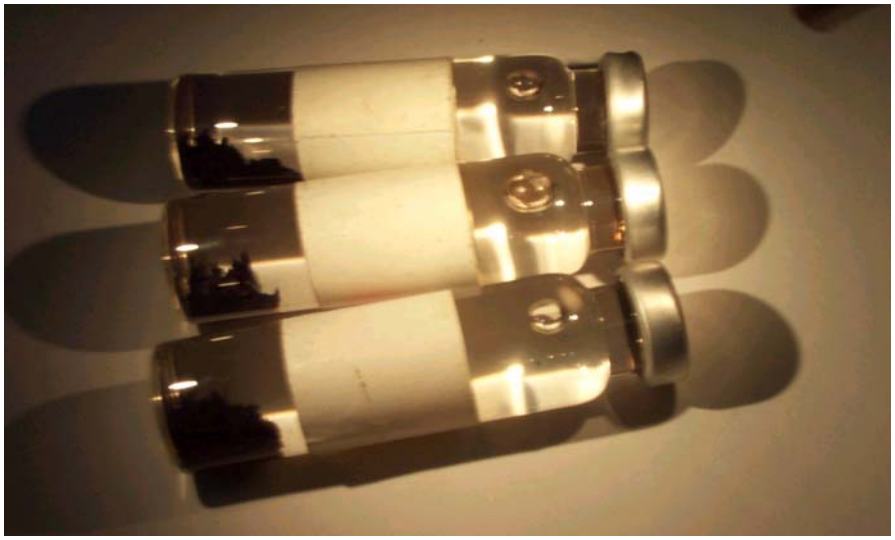

Figure 9. Visual confirmation of gaseous TCE breakdown by-products

Because there were no gas bubbles present in the control vials containing no iron, the possibility of air leaking in though the vial seal was unlikely. The gas bubble's presence was therefore attributed to the increased concentration of the volatile breakdown by-products of TCE and to the production of hydrogen. The instrumentation used to determine the concentration of TCE was also calibrated for the by-product ethene and the intermediate by-products cis-DCE, trans-DCE, 1,1-DCE, and vinyl chloride. The presence of intermediate by-products was confirmed by GC/FID, indicating that TCE degradation was occurring. The confirmed presence of ethene indicated that complete dehalogenation did occur when enough reaction time was provided. The absence of any by-products in the control vials containing no iron confirmed that the iron was responsible for the TCE degradation.

Effects of Acid-Wash Pretreatment on TCE Degradation Rates

The presence of precipitates on the surface of the iron can create a barrier that can hinder a TCE molecule from diffusing to the iron's reactive sites, resulting in decreased reaction rates. The iron samples studied were received in various forms and with different degrees of oxidation at the iron surface. When comparing rate constants for different iron samples, it was important to first remove any surface species and expose a clean iron surface.

The effect that acid washing has on TCE degradation rates can be seen in Figure 10.

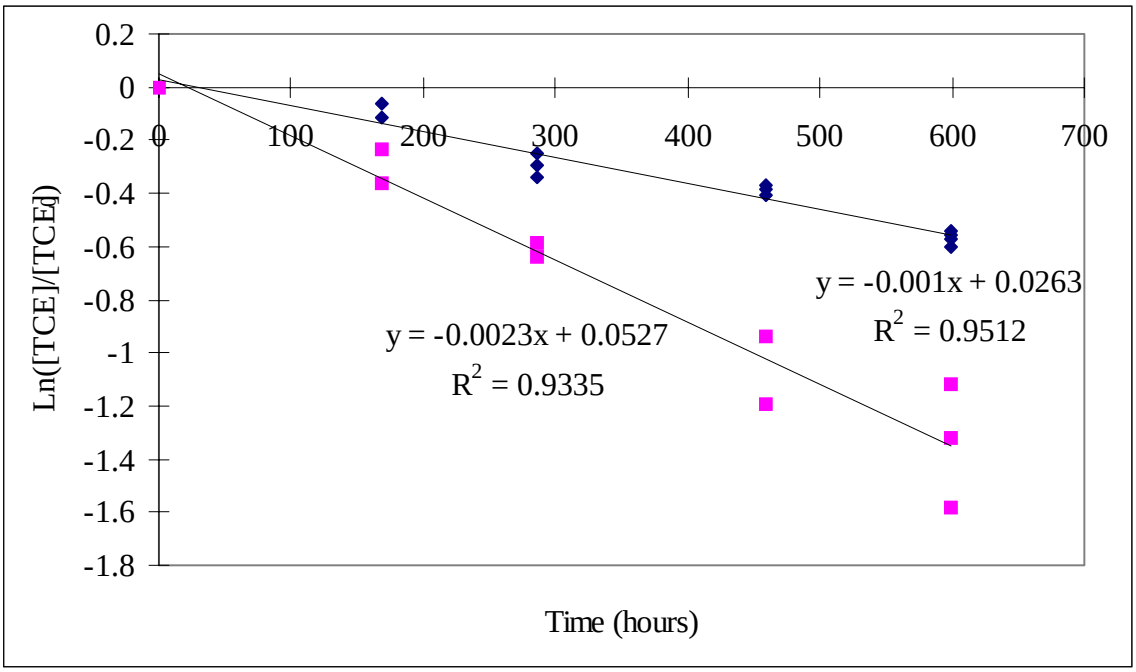

Figure 10. First order rate plots for acid washed and unwashed Connelly iron

The Connelly iron was set up in batch vial experiments as received and after acid washing. The slopes of the first order rate plots for the unwashed and the acid washed iron were normalized by mass and volume, resulting in k_{MV} values of 0.00010 L g^{-1} hr^{-1} and 0.00023 L g^{-1} hr^{-1} respectively. The rate constant for the acid washed iron was more than 100% greater than that of the unwashed iron. In order to eliminate the effects of surface species when comparing rate constants for different iron types, iron samples were acid washed before rate constants were obtained.

Another example of how surface species affect the reaction rate for a given iron type was encountered when comparing two types of iron received from Peerless Inc. The two types of iron, old Peerless and new Peerless, were obtained from the same manufacturing process and appeared to have similar particle size. Peerless Inc. stated that the new Peerless had received some additional treatment and should have been superior to the old Peerless at degrading TCE. Batch vial experiments were set up for both types of iron, as received and after acid washing. The first order rate plots obtained from the unwashed old and new Peerless iron are presented in Figures 11 and 12.

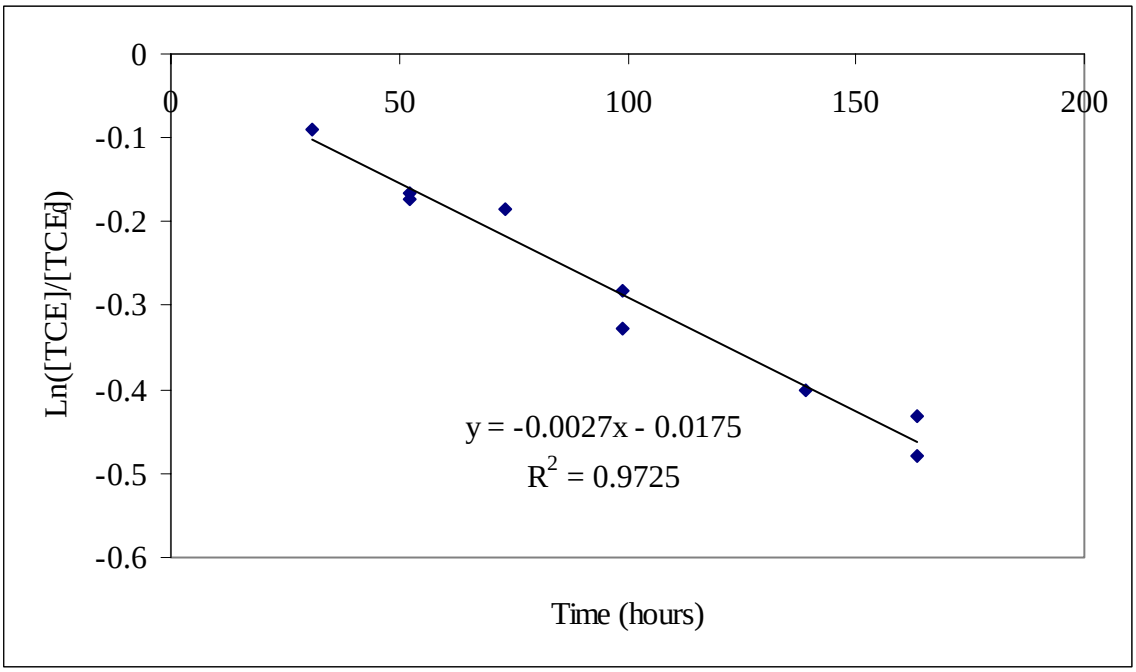

Figure 11. First order rate plot for unwashed old Peerless iron

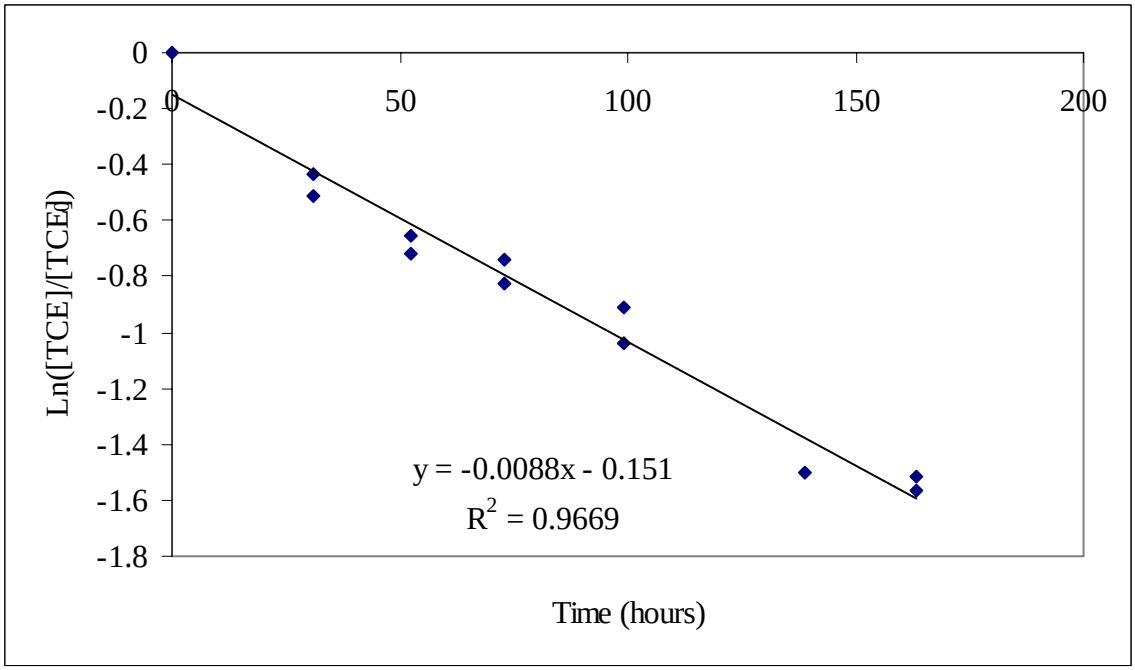

Figure 12. First order rate plot for unwashed new Peerless iron

The calculated k_{MV} values for the unwashed old and new Peerless were 0.000056 L g^{-1} hr^{-1} and 0.00018 L g^{-1} hr^{-1} respectively. The rate constant for the new Peerless was more than 200% greater than that of the old Peerless. Upon visual inspection of the two types of iron before testing, they seemed to have undergone different degrees of oxidation due to exposure to the atmosphere. The old Peerless had a greater amount of an orange precipitate on the surface than the new Peerless. To determine the effect that the presence of this precipitate had on degradation rates, batch vial experiments were set up using acid washed old and new Peerless iron. The first order rate plots obtained from acid washed old and new Peerless iron are presented in Figures 13 and 14.

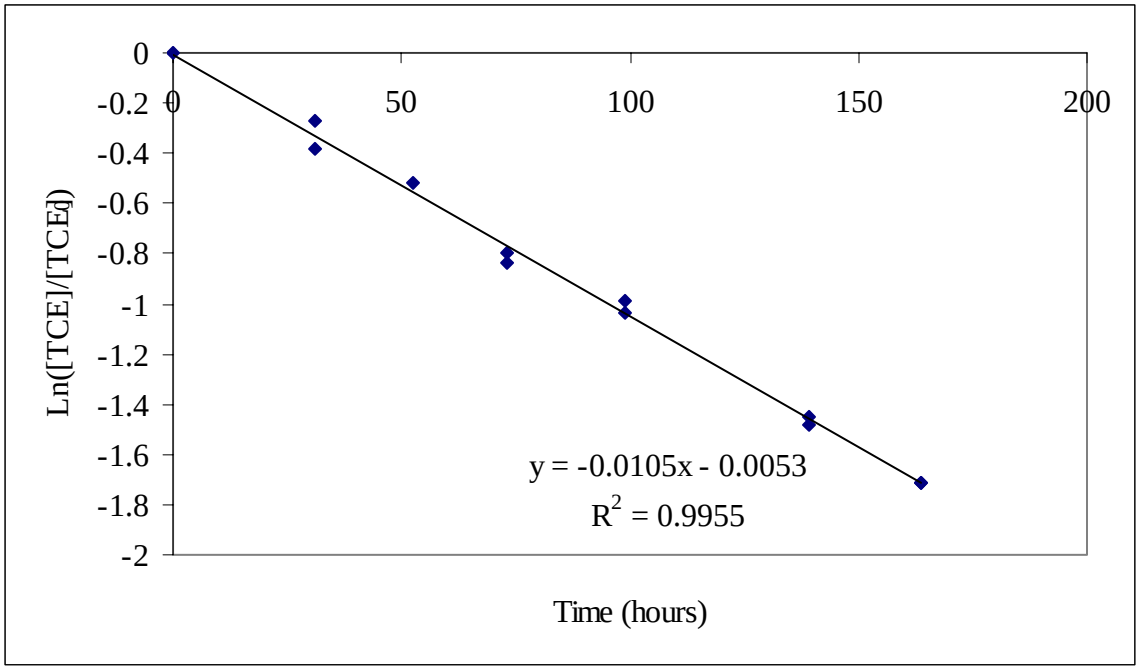

Figure 13. First order rate plot for acid washed old Peerless iron

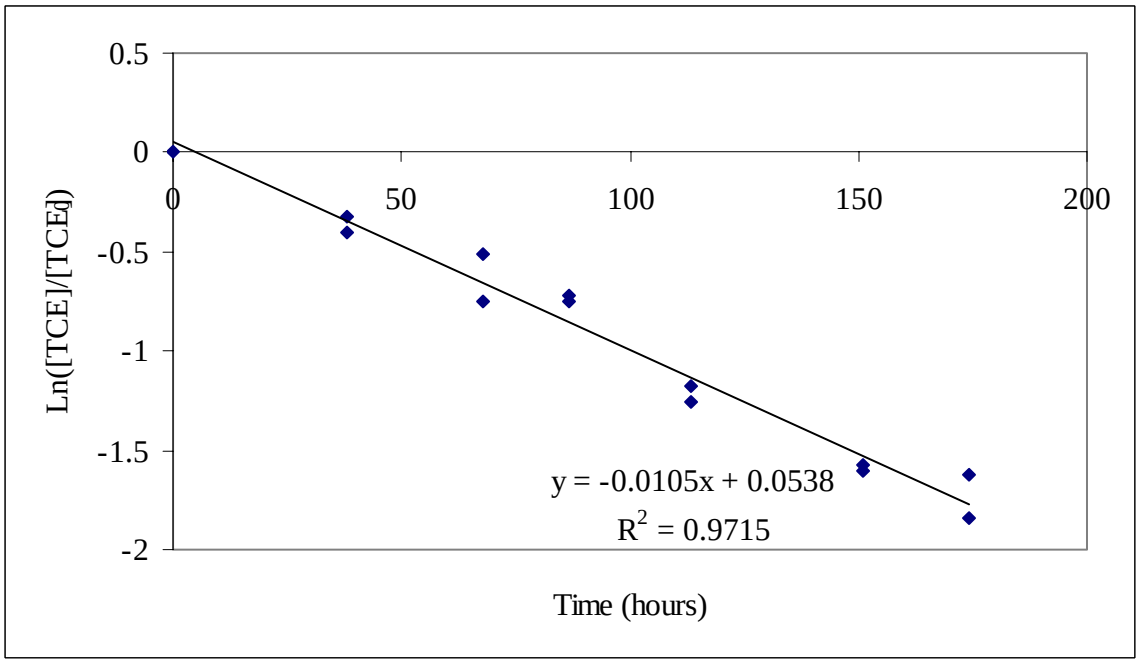

Figure 14. First order rate plot for acid washed new Peerless iron

The calculated k_{MV} values for the acid washed old and new Peerless were both 0.00021 L g^{-1} hr^{-1}. Acid washing the old Peerless promoted a 271% increased rate constant, compared to a 19% increase for the new Peerless. Clearly, acid washing was more beneficial to the reaction rate of the old Peerless than the new Peerless. Although the new Peerless was superior to the old Peerless when tested without pretreatment, the two iron types displayed identical reaction rates after the removal of oxide layers through acid washing. Apparently, the new Peerless iron was less susceptible to oxidation during shipping and storage. Therefore, any difference in the reaction rates of the two iron types was due to oxidation of the iron surface rather than differences in the inherent reactivity of the iron types.

Effects of Ultrasound Pretreatment on TCE Degradation Rates

The application of ultrasound to rejuvenate the surface of iron and restore TCE degradation rates has been used in both laboratory and field studies (Ruiz, 1998). The use of ultrasound to directly enhance the effectiveness of PRBWs after installation had positive results. This led to the investigation of the use of ultrasound as a pretreatment technique before installation.

Batch experiments were performed to compare the degradation rates of Connelly aggregate iron before and after subjection to 30 minutes of ultrasound. The first order rate plots obtained from the experiment are shown in Figures 15 and 16.

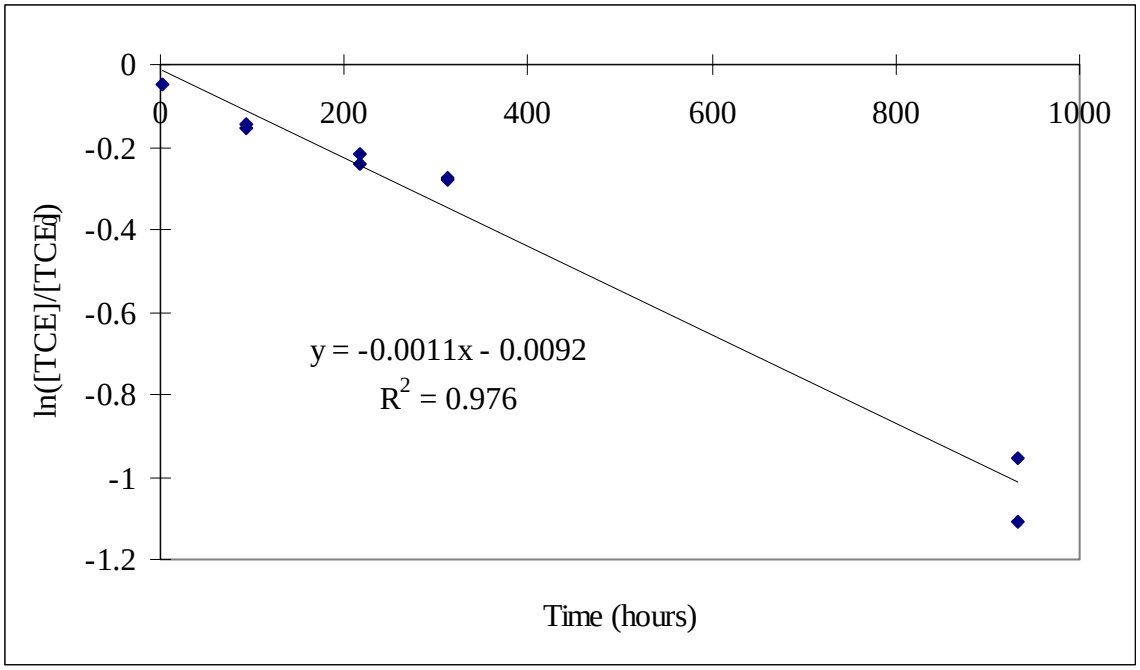

Figure 15. First order rate plot for Connelly aggregate iron with no ultrasound

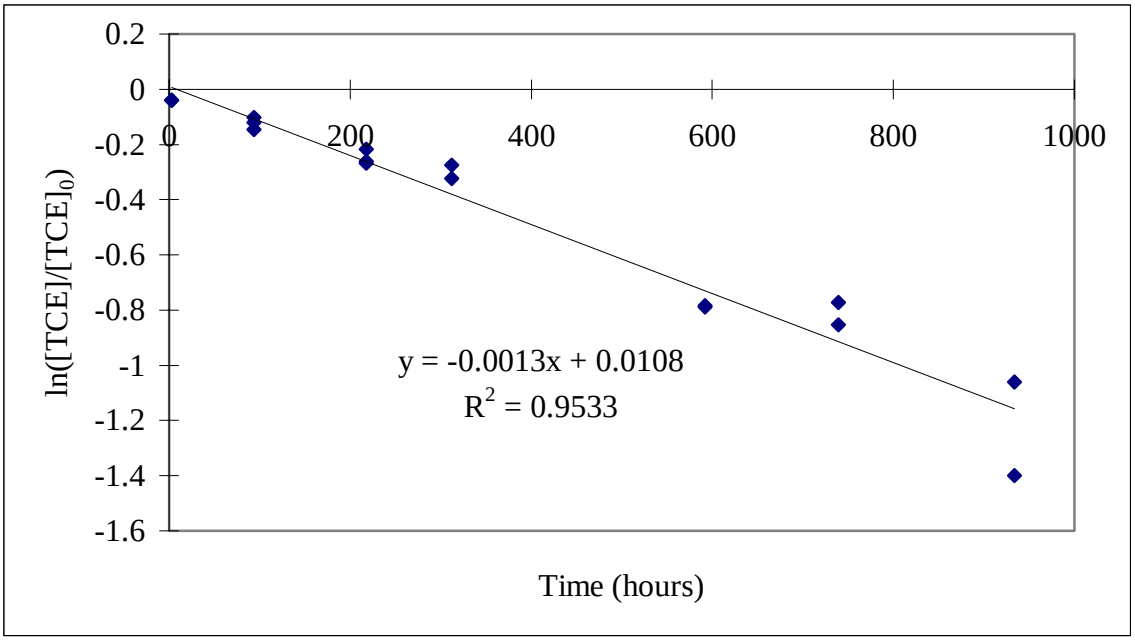

Figure 16. First order rate plot for Connelly aggregate iron after 30 minutes ultrasound

The calculated k_{MV} values for the untreated and the sonicated iron samples were 0.00011 L g^{-1} hr^{-1} and 0.00013 L g^{-1} hr^{-1} respectively. The sonication promoted an 18.2% increased rate constant for the Connelly iron sample. The ultrasound treatment had apparently exposed more of the iron surface by removing some of the oxide layer that had formed during exposure to air. Although the effects of ultrasound treatment were not as great as those for acid wash treatment with the same exposure time, ultrasound offers a practical application in the field on existing PRBWs.

The previous experiment involved surface species that formed during exposure to air. Additional experiments were performed to determine the effects that ultrasound had on precipitates that possibly form on the surface of the iron when exposed to conditions typically found in groundwater. The surface of granular iron is very irregular, containing many pores and crevices that contribute to the total surface area of the iron (Figure 17).

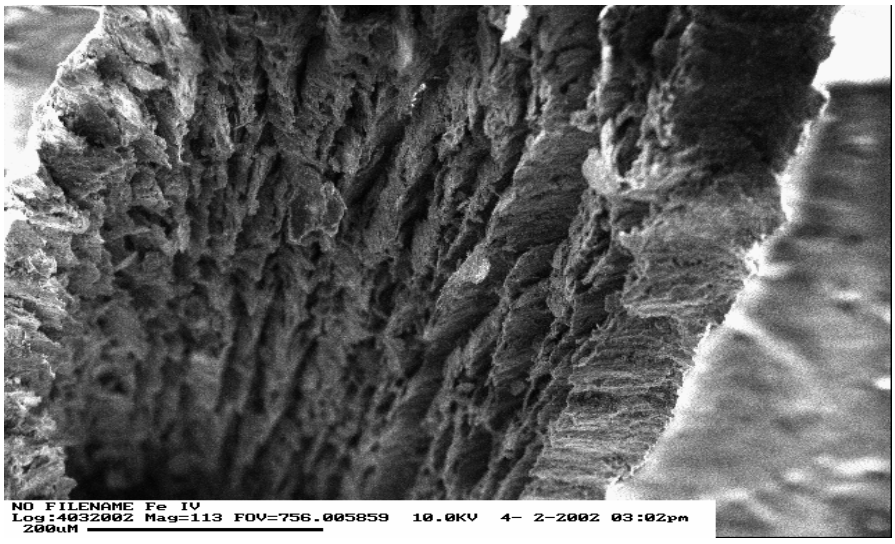

Figure 17. Scanning electron micrograph of granular iron surface

The formation of precipitates can prevent TCE from coming in contact with much of the iron surface, thus decreasing the iron's reactivity. Batch vial experiments were performed using Connelly iron that had been aged in an anaerobic saturated solution of calcium carbonate. Significant amounts of precipitate formation occurred during the aging process (Figure 18).

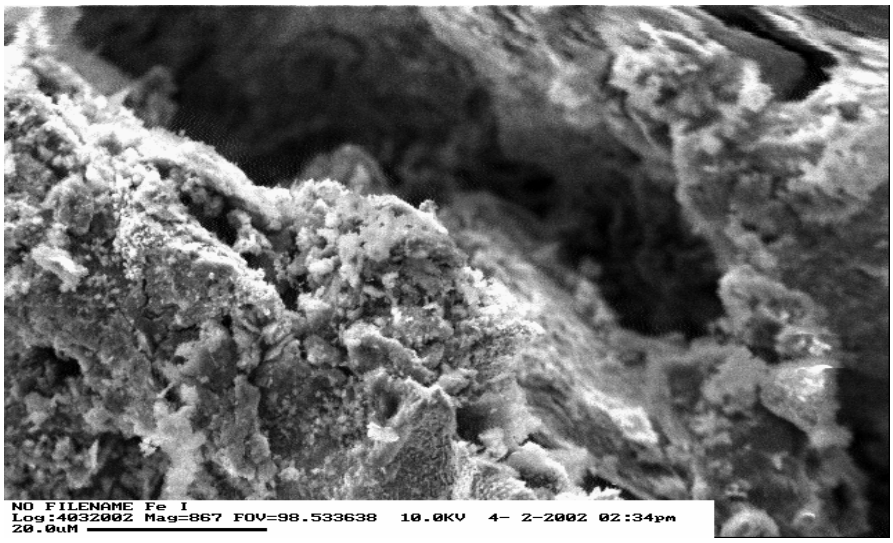

Figure 18. Scanning electron micrograph of precipitates on iron surface

The first order rate plot obtained for the aged Connelly iron is presented in Figure 19.

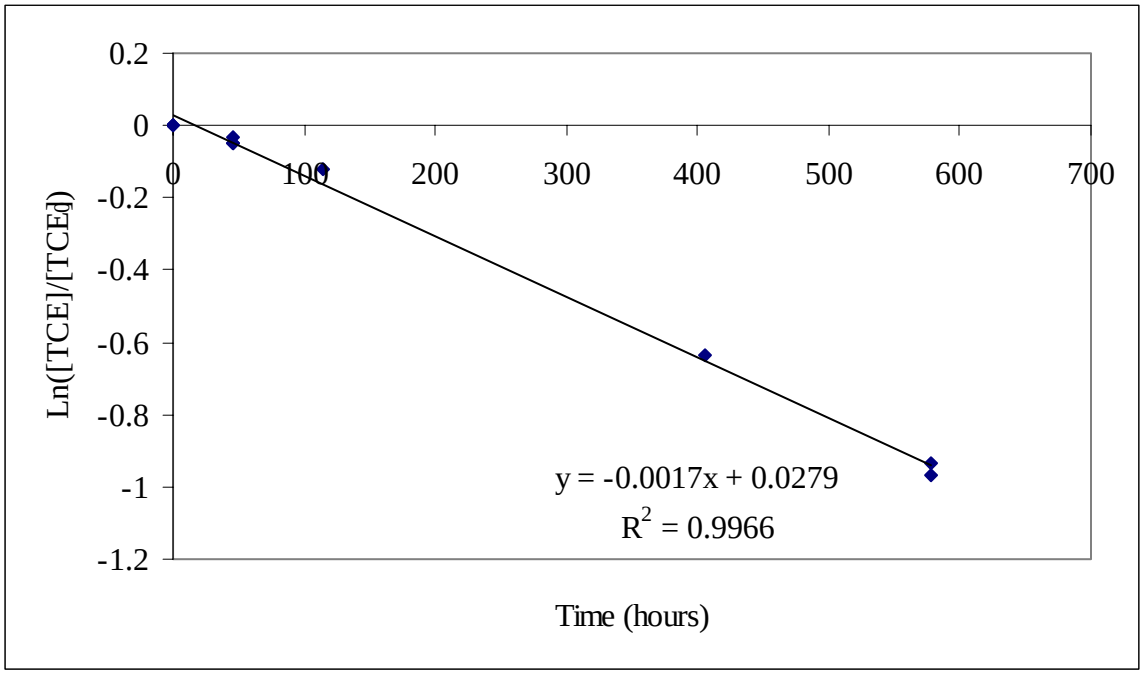

Figure 19. First order rate plot for Connelly iron aged in calcium carbonate solution

The calculated k_{MV} value for the aged Connelly iron was 0.000034 L g^{-1} hr^{-1}. The presence of the surface species that had formed during the aging process caused a significant decrease in the reaction rate. To test the effectiveness of ultrasound at removing these species, batch vial experiments were performed using aged Connelly iron that had also received ultrasound treatment. The first order rate plot obtained from this experiment is presented in Figure 20.

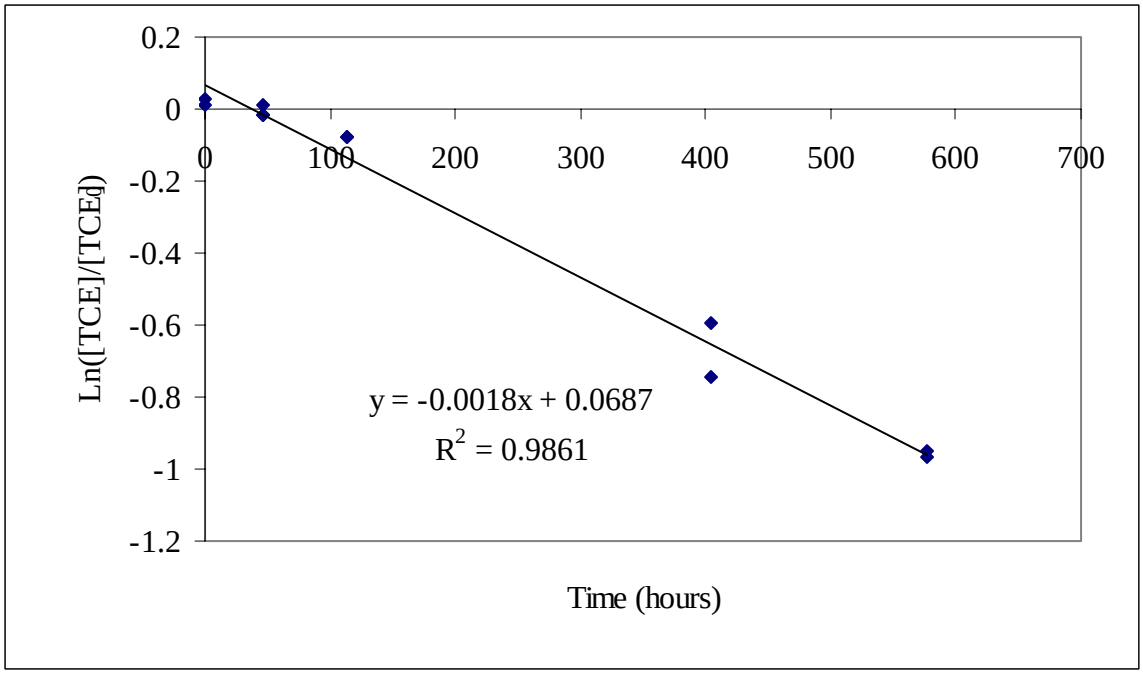

Figure 20. First order rate plot for aged Connelly iron after ultrasound treatment

The calculated k_{MV} value for the aged Connelly iron after ultrasound treatment was 0.000036 L g^{-1} hr^{-1}. The ultrasound treatment caused only a 5.9% increase in the rate constant. The precipitate layer that formed during the aging process was too thick for 30 minutes of ultrasound to be sufficiently effective. In the field, on existing PRBWs, a greater exposure time is employed, thus increasing the effectiveness of ultrasound treatment.

During this experiment, it was found that the effectiveness of ultrasound treatment varied between iron types. Batch vial experiments were performed using microscale iron. This iron was purchased from Alfa Aesar and had particle sizes ranging from 1-3 microns (Figure 21).

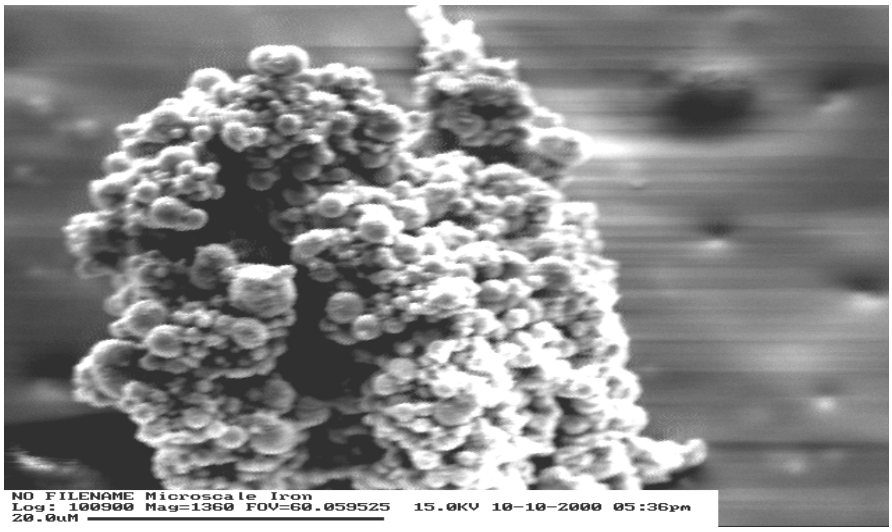

Figure 21. Scanning electron micrograph of microscale iron particles

The first order rate plots for aged microscale iron and aged microscale iron after ultrasound treatment are shown in Figures 22 and 23 respectively.

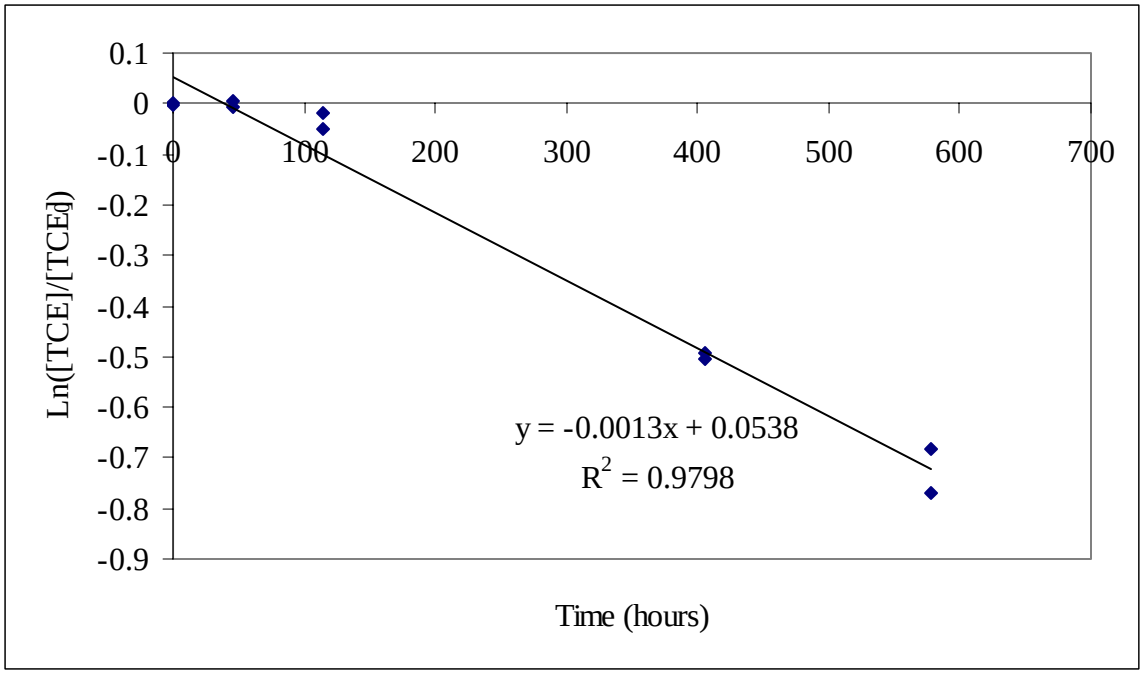

Figure 22. First order rate plot for microscale iron aged in calcium carbonate solution

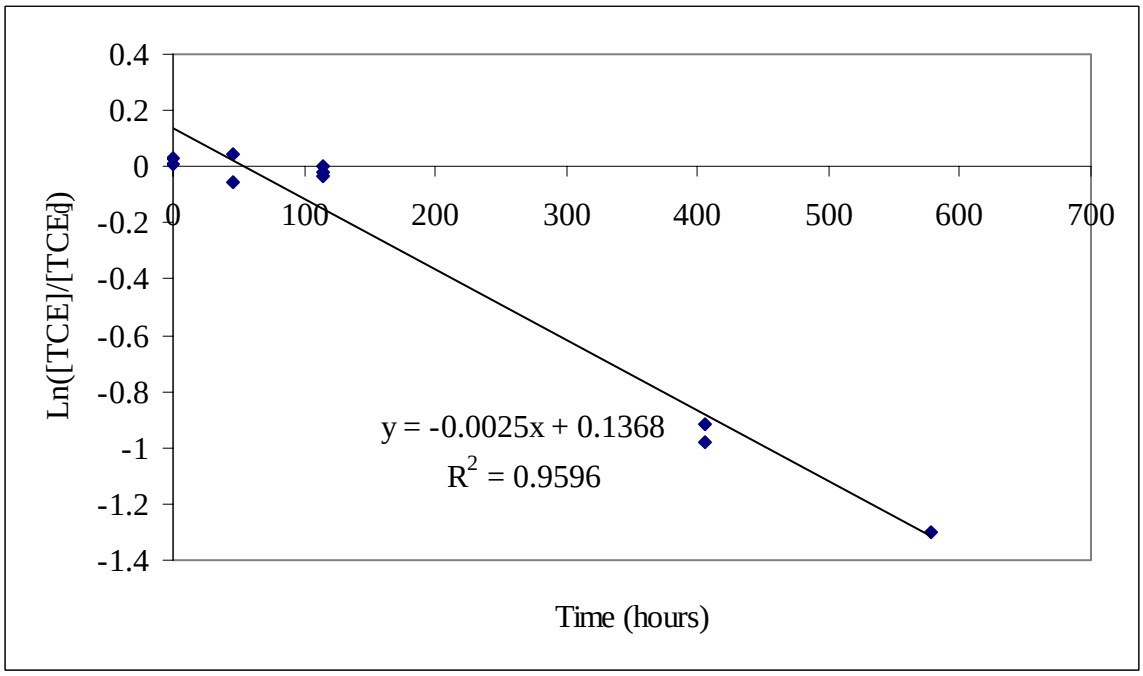

Figure 23. First order rate plot for aged microscale iron after ultrasound treatment

The calculated k_{MV} values for the aged microscale iron before and after ultrasound treatment were 0.000026 L g^{-1} hr^{-1} and 0.000048 L g^{-1} hr^{-1} respectively. The ultrasound treatment promoted an 84.6% increased rate constant. When compared to the 5.9% increase that the Connelly iron experienced after ultrasound treatment, the microscale iron appeared to be more affected. The larger Connelly particles created more of a dampening effect, making the ultrasound less effective. This can also be explained by the large differences in the surface areas of the two iron types. As the surface species were removed from the iron, a greater amount of surface area was exposed per amount of precipitate removed in the case of the microscale iron. This increase in exposed surface area is directly related to the increased rate constant observed for the microscale iron.

Normalization of TCE Degradation Rates by Mass

The normalization of rate constants by mass enables comparisons to be made between rate constants that were obtained using different amounts of iron. Batch experiments were performed using identical reaction vessels, varying only in the amount of iron present. The differences in rate constants were expected to be directly related to the amount of iron present, and once normalized by mass, should have been identical. Batch experiments were performed using 2 grams and 10 grams of Peerless iron and first order rate plots were obtained (Figures 24 and 25).

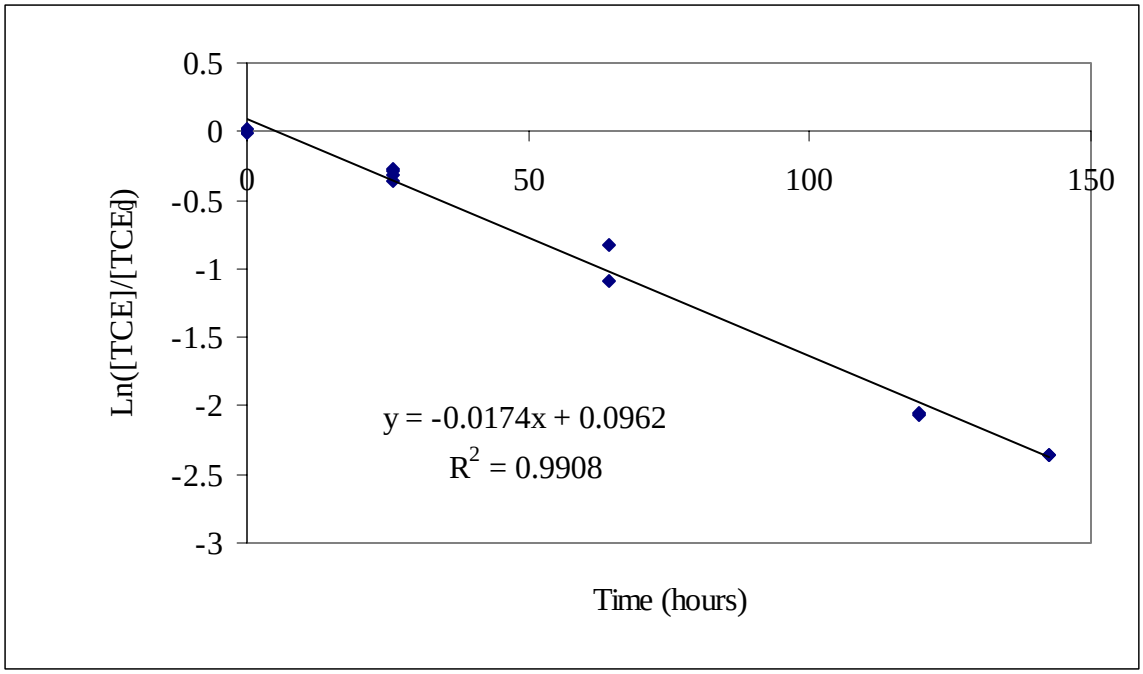

Figure 24. First order rate plot for batch experiment using 2 grams of Peerless iron

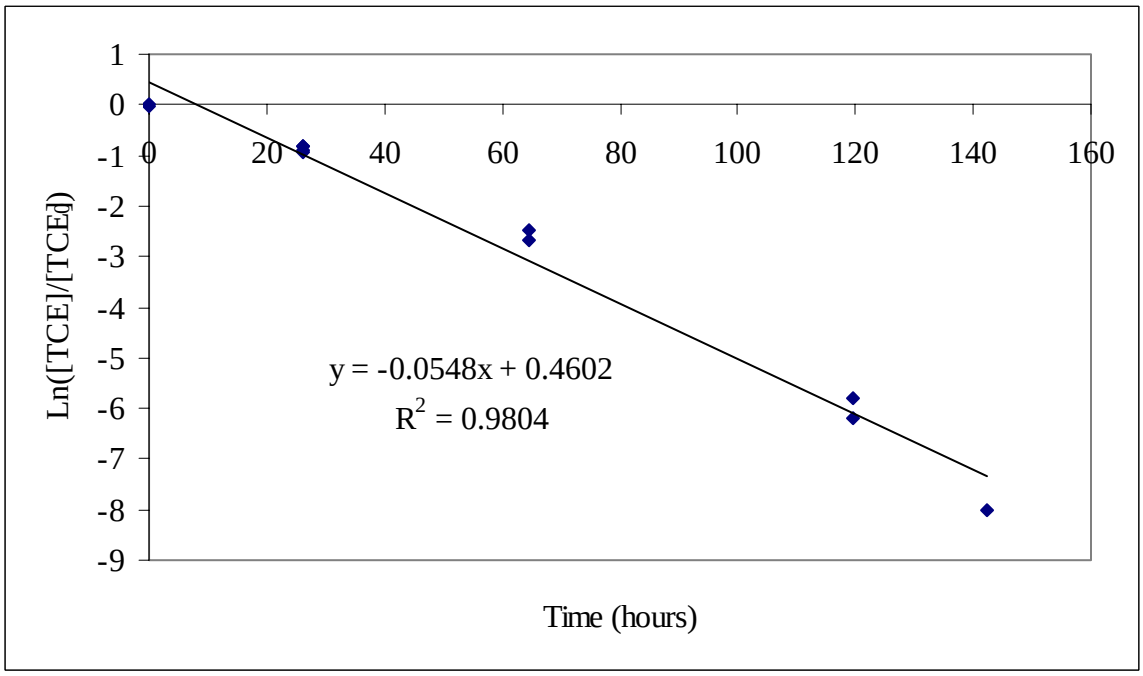

Figure 25. First order rate plot for batch experiment using 10 grams of Peerless iron

The calculated k_{MV} values for the experiments utilizing 2 grams and 10 grams of Peerless iron were 0.00035 L g^{-1} hr^{-1} and 0.00022 L g^{-1} hr^{-1} respectively. The normalized rate constants were not identical as was expected. Apparently, not all of the total iron surface area in the vials containing 10 grams of iron was participating in TCE degradation as efficiently as that of the vials containing 2 grams of iron. The difference can be attributed to several scenarios that possibly occurred as a result of the experimental setup. Although the vials were placed on a shaker table, the agitation was not enough to disperse the iron particles throughout the solution. Therefore, the iron particles remained at the bottom of the vials in a compact mass. This could have prevented adequate mixing of the solution, creating a concentration gradient of intermediate by-products within the iron mass. It has been well documented that DCE isomers reductively degrade at a much slower rate than TCE (Lau, 1998). Due to inadequate mixing, the DCE isomers that were initially formed by the reduction of TCE could have remained within the iron mass where they were further reduced to vinyl chloride and ethene. During this process, the DCE isomers would have been occupying reactive sites within the iron mass that would have been available for TCE reduction had a true solution been maintained. Basically, the diffusion of DCE isomers out of the iron mass and the diffusion of TCE molecules into the iron mass was hindered enough to create a concentration gradient, thus affecting the observed TCE degradation rate. Matheson and Tratnyek (1994) observed a similar trend of k_{MV} values decreasing with increased iron concentration. They demonstrated how

mixing intensity affects reaction rates, which is an indication of mass transport limited kinetics.

Normalization of TCE Degradation Rates by BET Surface Area

The reaction rate for the dehalogenation of TCE is dependent on the number of reactive sites available on the surface of the iron. When comparing the rates for two different iron types, the iron with a greater surface area generally has a faster rate. However, when these rates are normalized by surface area, any differences in reaction rate are due to differences in reactive site concentration. Since BET surface area measurements involve nonreactive sites as well as reactive sites, the reactive site concentration can be thought of as a ratio of reactive to nonreactive sites. The goal of this experiment was to determine differences in this ratio between different iron types. Any significant differences would indicate variations in composition or crystal structure of the iron types.

Batch vial experiments were performed using several different acid washed iron types. These iron types included old Peerless, new Peerless, Connelly (-8+50), Connelly (-30+70), Connelly (50 mesh), and nanoscale iron. The nanoscale iron had particle sizes in the range of 10-100nm (Figure 26).

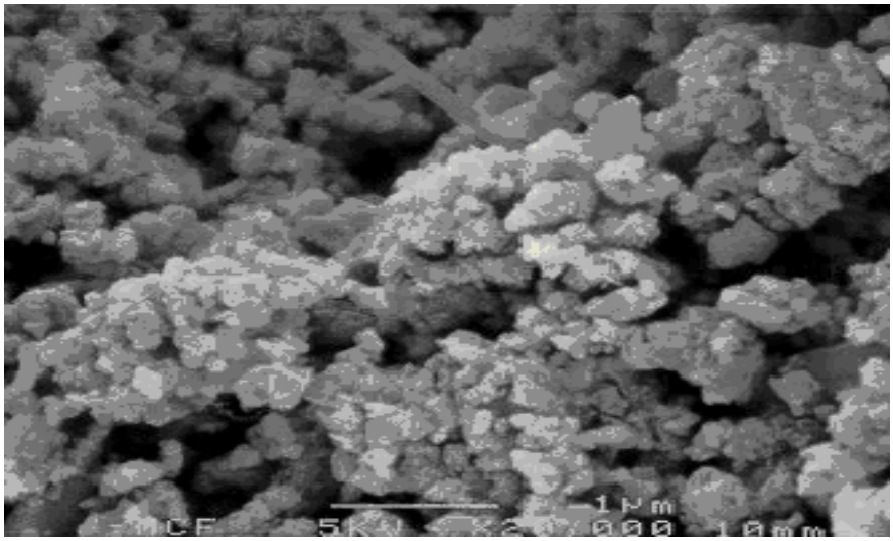

Figure 26. Scanning electron micrograph of nanoscale iron

Values for k_{MV} were obtained from the first order rate plots for each iron type. BET surface area analyses were also performed for each iron type by Peerless Inc. The measured surface area values were then used to calculate surface area normalized rate constants, k_{SA}.

The results are listed in table 3.

Table 3. Rate constants for various iron types normalized by surface area

Fe Type	k_{MV} (L g^{-1} hr^{-1})	Surface Area (m^2g^{-1})	k_{SA} (L $hr^{-1}m^{-2}$)
Old Peerless	0.00054	1.953	0.00027
New Peerless	0.00042	1.84	0.00023
Connelly (-8+50)	0.00044	1.838	0.00024
Connelly (-30+70)	0.00050	4.339	0.00011
Connelly (50 mesh)	0.00048	10.62	0.000045
Nanoscale	0.0016	62.297	0.000025

The normalized standard deviations for the slopes of the first-order regression lines are less than 0.00008 L g^{-1} hr^{-1}. As expected, the nanoscale iron, having the largest surface area, produced the largest value for k_{MV}. However, when the rate constants were normalized by surface area, the nanoscale iron produced the lowest k_{SA} value. This shows that the high reaction rates achieved by the nanoscale iron are a result of its high surface area. The low k_{SA} value obtained for the nanoscale iron could be the result of several compositional and structural characteristics of nanoparticles. These characteristics include reactive site concentration, the presence of a passivating shell, and the aggregation of nanoparticles in solution.

Since the surface area analysis measures reactive as well as nonreactive sites, it is possible that not all of this measured surface area participates in TCE degradation. It is at

these nonreactive sites where sorption of TCE molecules can occur without any reduction taking place. The low k_{SA} value for the nanoscale iron could indicate the presence of a low ratio of reactive to nonreactive sites. However, due to the nanoscale iron's high surface area, the large number of reactive sites present per gram would still result in a high k_{MV} value.

The presence of a passivating layer on the surface of the iron nanoparticles could also explain the low values obtained for k_{SA}. Metallic iron nanoparticles have been characterized in recent literature through the use of various spectroscopy and microscopy techniques including Transmission Electron Microscopy, X-ray Photoelectron Spectroscopy, X-ray Diffraction, and Scanning Transmission X-ray Microscopy (Nurmi et al., 2005). The results revealed that nanoscale iron particles synthesized by reductive precipitation with $NaBH_4$ consist of an iron core with a shell that is composed of iron and boron oxides. If the reactivity of the nanoparticles is dependent on the oxidation of the iron core, then charge and mass transport across this oxide, passivating layer could affect the kinetics of TCE reduction. If the transport across the shell boundary were rate limiting, that would explain the low observed value for k_{SA}.

Another possible explanation for the low observed k_{SA} values of the nanoscale iron involves the values for the specific surface area that were used to normalize the rate constants. Reactive nanoparticles have a strong tendency to aggregate in solution. The reactive surface area of highly aggregated nanoparticles suspended in solution is likely to be very different from the surface area measured on dry, dispersed nano-sized powders (Nurmi et al., 2005). Surface area values that were used to normalize rate constants could

have been much larger than the actual surface area of the aggregated nanoparticles in solution. This would result in a lower calculated value for k_{SA}.

Comparison of TCE Degradation Rates for Different Iron Types

Several different iron types were obtained from Peerless, Inc., including iron containing 1% copper, fine gray iron, and Peerless iron (size –8+50). Batch vial experiments were performed for each new iron type and for Connelly iron (size-8+50) and nanoscale iron. Crimp top, 20 mL glass vials equipped with Teflon septa were used during this experiment. Since the solution volume was reduced from 40 mL to 20 mL, the amount of iron was reduced from 2 grams to 1 gram to maintain manageable reaction rates.

The first order rate plots obtained for each iron type are presented in Figures 27 through 31.

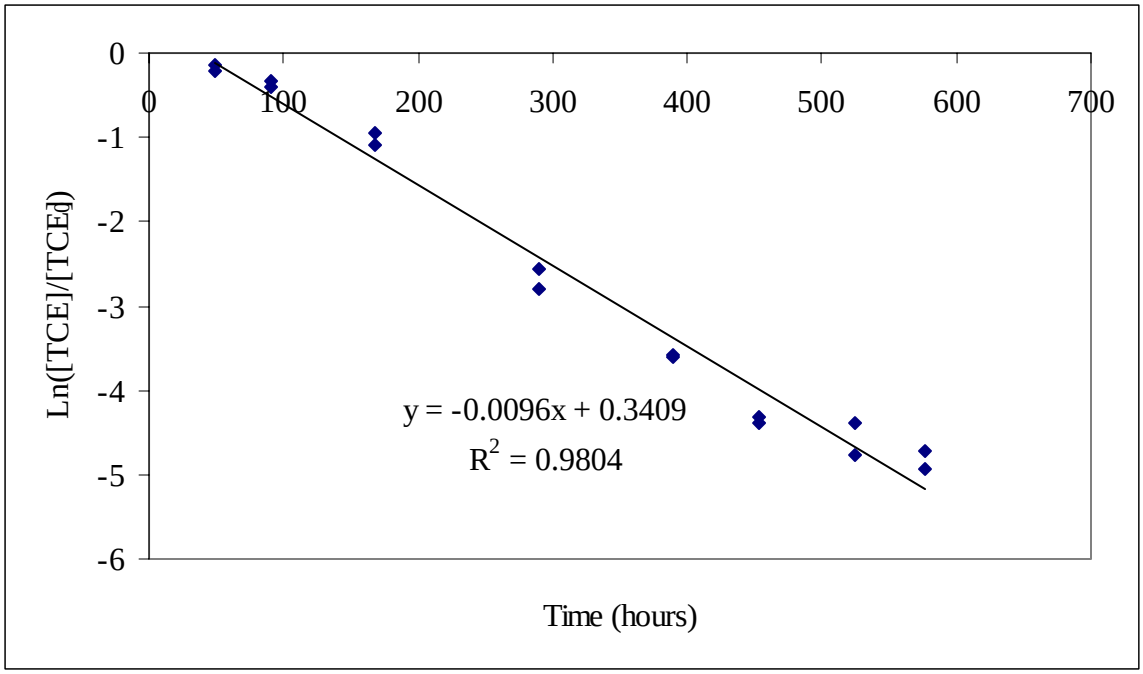

Figure 27. First order rate plot for 1 gram Peerless Fe + 1%Cu using 20mL vials

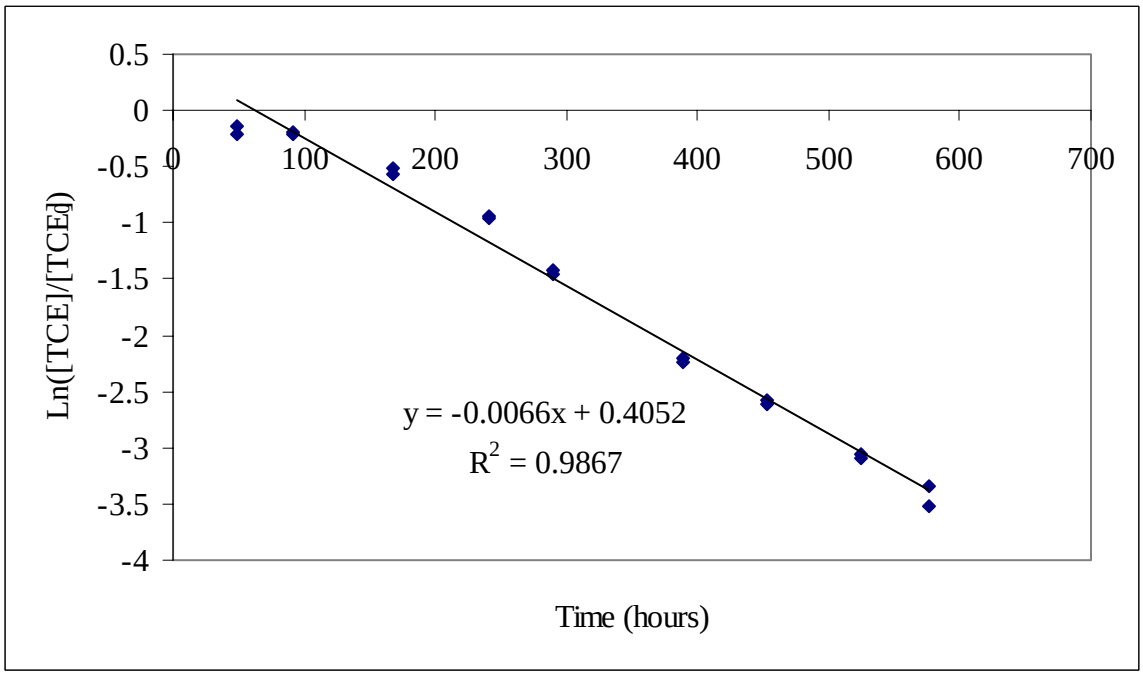

Figure 28. First order rate plot for 1 gram Peerless fine gray iron using 20mL vials

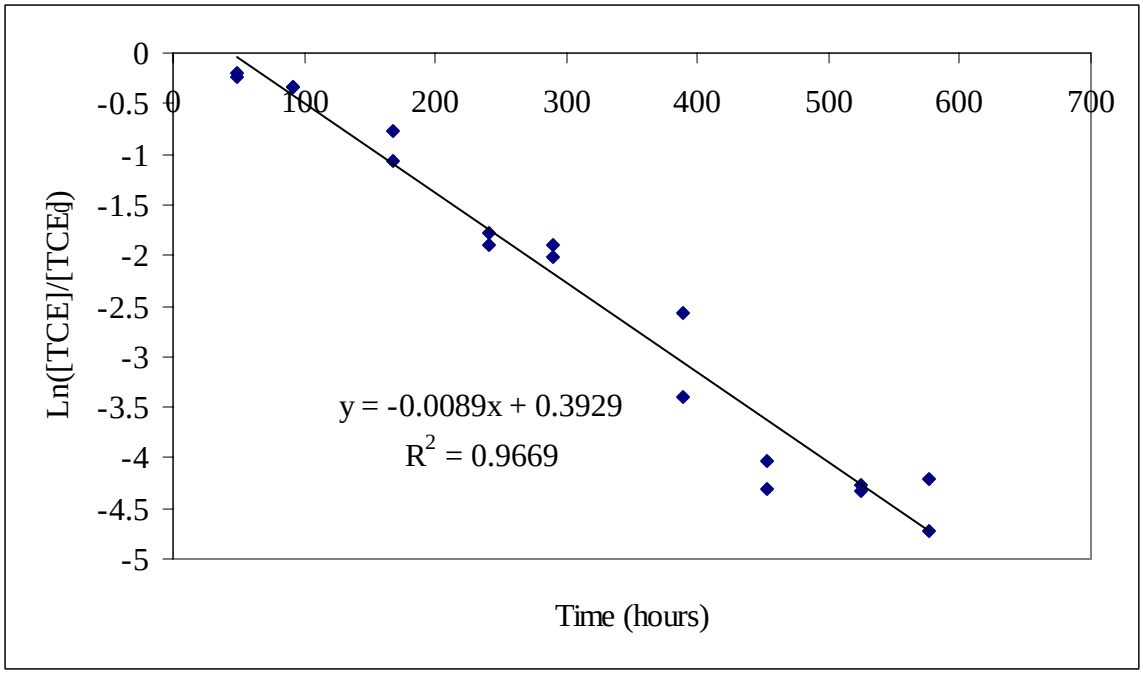

Figure 29. First order rate plot for 1 gram Peerless iron (size –8+50) using 20mL vials

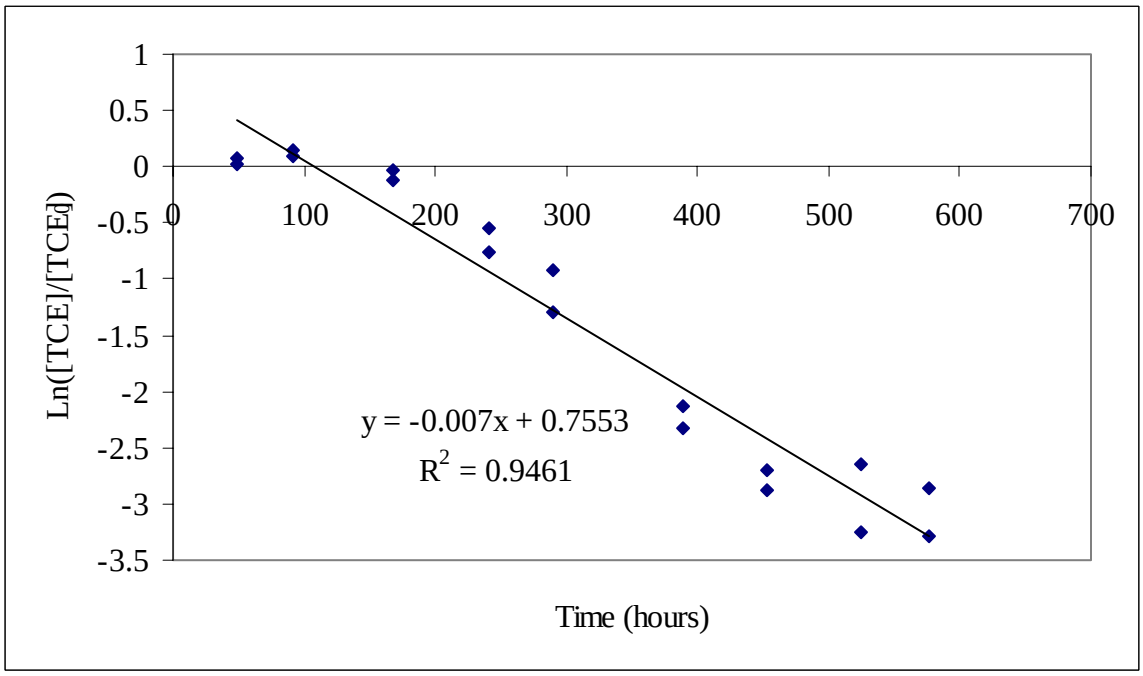

Figure 30. First order rate plot for 1 gram Connelly iron (size –8+50) using 20mL vials

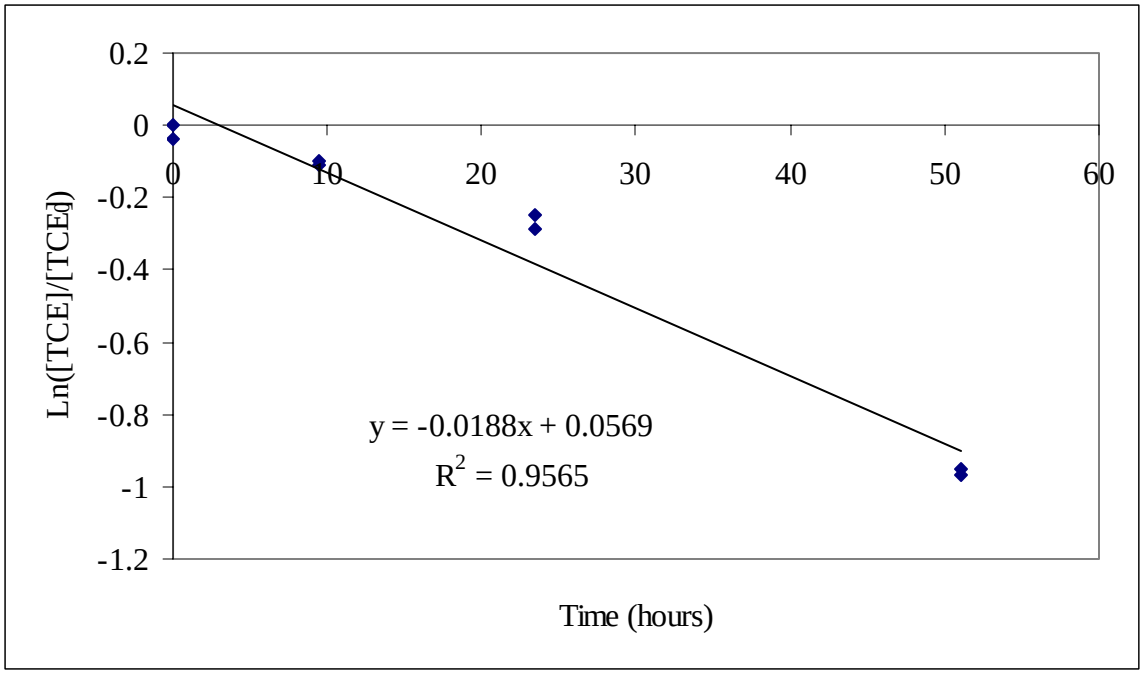

Figure 31. First order rate plot for 1 gram nanoscale iron using 20 mL vials

The rate constants were obtained from the slopes of each linear equation, normalized by iron mass and solution volume, and are presented in Table 4.

Table 4. First order rate constants obtained using 1 gram iron in 20 mL crimp top vials

Iron type	k_{MV} (L g^{-1} hr^{-1})
Peerless Fe +1% Cu	0.00019
Peerless fine gray Fe	0.00013
Peerless Fe (size –8+50)	0.00018
Connelly Fe (size –8+50)	0.00014
Nanoscale Fe	0.00038

The normalized standard deviations for the slopes of the first-order regression lines are less than 0.0000038 L g^{-1} hr^{-1}. The Peerless iron +1% Cu, producing a k_{MV} value of 0.00019 L g^{-1} hr^{-1}, was the most effective of all the commercially available iron types at degrading TCE. The nanoscale iron produced in the laboratory was superior to all other iron types, as seen before in previous experiments. The Peerless fine gray iron, producing a k_{MV} value of 0.00013 L g^{-1} hr^{-1}, was the least effective of all the commercially available iron types in this experiment. Iron samples with the same particle size from two different manufacturers were compared in this experiment. The Peerless iron (size –8+50) and the Connelly iron (size –8+50) produced k_{MV} values of 0.00018 L g^{-1} hr^{-1} and 0.00014 L g^{-1} hr^{-1}, respectively. The rate constant for the Peerless iron was 28% greater than that for the Connelly iron with the same particle size.

It is important to note that although the rate constants obtained in this experiment were normalized by mass and volume, they should not be compared directly to previously obtained rate constants using different reaction vials. The vials used in this experiment were 20 mL, and 40 mL vials were used in previous experiments. This difference can be accounted for through the normalization of rate constants by volume. However, because the two types of vials differ in their construction, related to the procedure used to seal them, other variables could exist.

To explore the possibility that the 20 mL vials were different from the 40 mL vials in ways other than just solution volume, the rate constant for the Connelly iron (size –8+50) was obtained using 40 mL vials. A batch vial experiment was performed using 2

grams of Connelly iron (size –8+50) per 40 mL vial. The first order rate plot for this experiment was obtained (Figure 32).

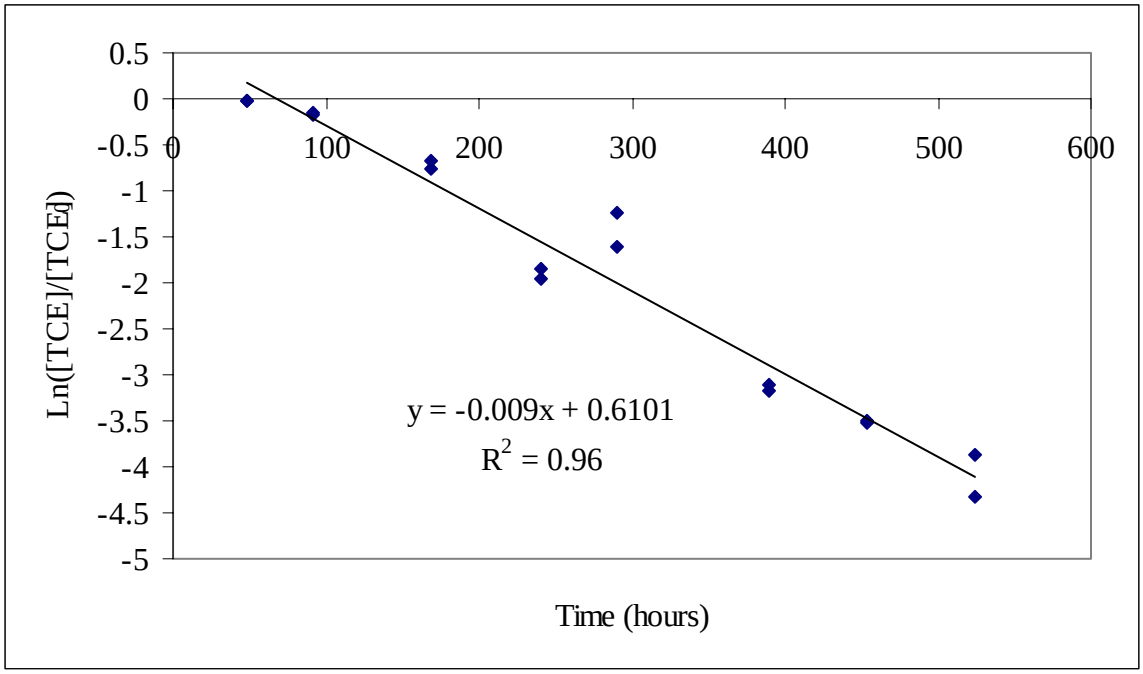

Figure 32. First order rate plot for 2 grams Connelly iron (size –8+50) using 40 mL vials

The rate constant for the 2 grams iron/40 mL vial experiment can be directly compared to the rate constant for the 1 gram iron/20 mL vial experiment after normalization by mass and volume. These k_{MV} values were 0.00018 L g^{-1} hr^{-1} and 0.00014 L g^{-1} hr^{-1} respectively. A 28.6% greater rate constant was obtained using the 40 mL vials. This indicated that some difference other than solution volume existed between the two vial types. After investigating the loss of TCE in control vials, due to volatilization, it was found that the two vial types were indeed different. It was found that during the same amount of time,

the screw cap 40 mL control vials exhibited a greater decrease in TCE concentration than the 20 mL crimp top control vials. This would account for the greater rate constant reported for the 40 mL vials. The decreased TCE concentration in control vials was attributed to mechanical problems associated with the screw caps. The amount of force used to tighten the caps could distort the seal, thus causing some leakage. In contrast, the crimp top vials utilize a specialized tool that distributes the crimping force equally around the septum, promoting a better seal.

Conclusions

Summary of Objectives

The experimental procedure used in this study produced linear first order rate plots from which dehalogenation rate constants were obtained. The pretreatment techniques employed in this study demonstrated a beneficial effect by removing oxide precipitates from the iron surface, thus increasing the reactivity of the iron. Acid washing iron particles was applied as a standard procedure to ensure that a clean iron surface, free from the effects of oxidized species, was being tested. Mass loading studies demonstrated how physical factors involved with a large amount of iron per sample vial could affect the observed TCE degradation reaction rates. Therefore, comparisons of k_{MV} values should only be made when obtained using the same amount of iron per sample vial. Surface area studies confirmed that the smaller iron particles, such as the nanoscale iron, have a greater surface area per unit mass. The large rate constant, k_{MV}, obtained for

the nanoscale iron was a result of this high surface area. However, the calculated surface area normalized rate constant, k_{SA}, for the nanoscale iron was significantly lower than those for the granular iron samples tested. It was concluded that differences in surface area normalized rate constants, between different iron particle types, could be attributed to inherent characteristics of the iron, such as composition and crystal structure.

Future Recommendations

Future batch vial experiments should utilize crimp-top vials due to the decreased loss of TCE attributed to volatilization. A different method of mixing the vials should be investigated to further understand the effects of mass loading. Based on the positive results of the bi-metallic iron/copper particles, future studies should involve rate experiments using other bi-metallic particles such as iron/zinc and iron/magnesium.

LIST OF REFERENCES

Adamson, A.W. In *Physical and Chemistry of Surface.* 5th ed. John Wiley & Sons: New York, 1990.

Brooks, K. Master's Thesis, University of Central Florida, Fall 2000.

Gilham, R.W.; Burris, D.R. Proceedings from Subsurface Restoration Conference, The Third International Conference on Ground Water Quality, Dallas TX, June, 1992.

Gilham, R.W.; Hannesin S.F. Presentation at Modern Trends in Hydrogeology; the Conference of the Canadian National Chapter, International Association of Hydrologists, Hamilton, Ontario, Canada, May, 1992.

Gilham, R.W.; Hannesin S.F.; Orth, W.S. Presentation at the Haz Mat Central Conference, Chicago IL, March ,1993.

Gilham, R.W.; Hannesin, S.F. *Ground Water* 1994, 32, 958-967.

Gotpagar, J.K.; et al. *Journal of Haz. Mat*. 1998, 62, 243-264.

Hunt, J.R.; Sitar, N.; Udell, K.S. *Water Resources Research* 1988, 24, 1274-1258.

Johnson, T. L.; Tratnyek, P.G. Preprinted extended abstract, presented before the Division of Environmental Chemistry, American Chemical Society, Anaheim, CA, April, 1995.

Lau, N. Master's Thesis, University of Central Florida, Summer 1998.

Mackenzie, P.D.; Sivavec, T.M.; Horney, D.P. International Containment Technology Conference and Exhibition, St. Petersburg, FL, February , 1997.

Matheson, L.J.; Tratnyek, P.G. *Environ. Sci. and Tech.* 1994, 28, 2046 - 2053.

Nurmi, J.T.; Tratnyek, P.G.; et al. *Environ. Sci. and Tech.* 2005, 39, 1221-1230.

Nyer, E.; et al. *In Situ Treatment Technology*. Lewis: New York, 1996.

Orth, S.W.; Gillham, R.W. *Environ. Sci. and Tech*, 1996, 30, 66.

Ruiz, N.E. Ph.D. Dissertation, University of Central Florida, Spring 1998.

Shiau, B.; Sabatini, D.A.; Harwel, J.H. *Groundwater* 1994, 32, 561-569.

Sivavec, T. M. et al. International Containment Technology Conference and Exhibition, St. Petersburg, FL, February, 1997.

Title 40 Code of Federal Regulations, 1998 parts 131-136.

Toy, P. Master's Thesis, University of Central Florida, Summer 1998.

Udell, K.S. Annual Review of Heat Transfer 1996, 7, 333-405.

Vogel, T.M.; Cridle, C.S.; McCarty, P.L. *Environ. Sci. and Tech.* 1987, 21,722-736.

Wang, C.B.; Zhang,W.X.; *Environ. Sci. Tech.* 1997, 31, 2154-2156.

Zhou, M.; Rou, D.R.; *Environ. Sci. & Tech*. 2000, 34, 1985-1990.